Multiomics and digital monitoring during lifestyle changes reveal independent dimensions of human biology and health

Francesco Marabita[1,2], Tojo James[1,2], Anu Karhu[1], Heidi Virtanen[1], Kaisa Kettunen[1,6], Hans Stenlund[3], Fredrik Boulund[4], Cecilia Hellström[5], Maja Neiman[5], Robert Mills[1], Teemu Perheentupa[1], Hannele Laivuori[1,7,8],Pyry Helkkula[1], Myles Byrne[1], Ilkka Jokinen[1], Harri Honko[9], Antti Kallonen[9], Miikka Ermes[10], Heidi Similä[10], Mikko Lindholm[10], Elisabeth Widen[1], Samuli Ripatti[1], Maritta Perälä-Heape[11,12], Lars Engstrand[4], Peter Nilsson[5], Thomas Moritz[3,13], Timo Miettinen[1], Riitta Sallinen[1,2], Olli Kallioniemi[1,2]

[1]Institute for Molecular Medicine Finland (FIMM), HiLIFE, University of Helsinki, Helsinki, Finland. [2]Science for Life Laboratory, Department of Oncology-Pathology, Karolinska Institutet, Stockholm, Sweden. [3]Science for Life Laboratory, Swedish Metabolomics Centre, Department of Forest Genetics and Plant Physiology, Swedish University of Agricultural Sciences, Umeå, Sweden. [4]Science for Life Laboratory, Center for Translational Microbiome Research, Department of Microbiology, Tumor and Cell biology, Karolinska Institutet, Stockholm, Sweden. [5]Science for Life Laboratory, Division of Affinity Proteomics, Department of Protein Science, KTH Royal Institute of Technology, Stockholm, Sweden. [6]HUS Diagnostic Center, Laboratory of Genetics, University of Helsinki and Helsinki University Hospital, Helsinki, Finland. [7]Medical and Clinical Genetics, University of Helsinki and Helsinki University Hospital, Helsinki, Finland. [8]Department of Obstetrics and Gynecology, Tampere University Hospital and Tampere University, Faculty of Medicine and Health Technology, Tampere, Finland. [9]Tampere University of Technology, Tampere, Finland [10]VTT Technical Research Centre of Finland, Espoo, Finland. [11]Faculty of Medicine, University of Oulu, Oulu, Finland. [12]Centre for Health and Technology, University of Oulu, Oulu, Finland. [13]Novo Nordisk Foundation Center for Basic Metabolic Research, Faculty of Health and Medical Sciences, University of Copenhagen, Copenhagen, Denmark.

Abstract

In order to explore opportunities for personalized and predictive health care, we collected serial clinical measurements, health surveys and multiomics profiles (genomics, proteomics, autoantibodies, metabolomics and gut microbiome) from 96 individuals. The participants underwent data-driven health coaching over a 16-month period with continuous digital monitoring of activity and sleep. Multiomics factor analysis resulted in an unsupervised, data-driven and integrated view of human health, revealing distinct and independent molecular factors linked to obesity, diabetes, liver function, cardiovascular disease, inflammation, immunity, exercise, diet and hormonal effects. The data revealed novel and previously uncovered associations between risk factors, molecular pathways, and quantitative lifestyle parameters. For example, ethinyl estradiol use had a distinct impact on metabolites, proteins and physiology. Multidimensional molecular and digital health signatures uncovered biological variability between people and quantitative effects of lifestyle changes, hence illustrating the value of the combined use of molecular and digital monitoring of human health.

Longitudinal measurements of clinical laboratory tests, multiomics profiles, and digital health monitoring using wearable sensors could facilitate a comprehensive analysis of human health and the impact of lifestyle and disease. This provides opportunities to explore human systems biology and to predict and intervene in processes leading to disease. However, our ability to make use of such data and define actionable insights, correlations and causal patterns is limited. There is a shortage of deep integrated datasets, where different dimensions of human biology have been explored at the same time and their changes over time recorded and/or connected with digital monitoring data from wearable devices. Each individual has a unique profile, composed of genetic, epigenetic, molecular, clinical and lifestyle parameters, which may change over time during development, aging and disease transitions. These processes cannot be understood as a single general pathway for the average human or patient, but they can be better described as a collection of individual health trajectories, where changes in individual variables are highly interconnected. Several studies have investigated the use of individualized molecular profiles to assess disease risks or the connection between omics measurements and clinical tests, using an n-of-one longitudinal approach[1,2], a cross-sectional design[3], a controlled longitudinal perturbation study[4], and a cohort study with personal behavioural coaching[5]. More recently, other studies[6-8] have analysed longitudinal data over an extended time period in a cohort of individuals at risk for diabetes, while another prospective observational study investigated the stability of the individual molecular signatures[9].

The Digital Health Revolution (DHR) program[10] was based on the concept that future healthcare strategies will evolve in a direction which allows citizens to control and make use of their personal data to improve their health and wellness. The project aimed at implementing proactive P4 healthcare (predictive, preventive, personalized, and participatory), with multi-level molecular and digital data. Within this framework, we integrated deep multiomics profiles and connected them to health surveys, clinical observations and digital health measurements. We aimed to 1) integrate longitudinal multi-omics and digital health data between and within people over time to reveal subgroups and personal trajectories; 2) exploit the discovered associations to understand novel links between molecular, clinical and digital health data and 3) verify if data feedback and coaching would guide and motivate

people to undertake lifestyle changes. Overall, we aimed at achieving a holistic understanding of the parameters involved in different aspects of human biology and health. To accomplish these goals, we applied multiomics factor analysis and then connected the learned factors with interpretable characteristics of health and behaviour as well as quantitative digital health data.

Results

Study overview

We carried out a 16-month longitudinal study on 96 individuals (aged 25-59) recruited from an occupational healthcare clinic in Helsinki, Finland (Supplementary Figure 1-2 and Supplementary Table 1). The participants had no previously diagnosed serious chronic diseases, although we allowed individuals with risk factors for chronic diseases to participate. We acquired comprehensive measurements of health and behaviour, including anthropometrics, clinical laboratory tests, questionnaire data, physical fitness tests, and activity and sleep quantification with a wearable device. In addition, we performed a series of omics measurements to study the genome, the plasma proteome and metabolome, the autoantibody profile and the gut microbiome. The prospective collection of molecular and digital profiles resulted in a thorough longitudinal dataset of human health and lifestyle (Figure 1). We defined baseline molecular profiles and longitudinal data trajectories in the participants during personalized lifestyle coaching. We collected over 20,000 biological samples during five study visits and generated a compendium of >53 million primary data points for 558,032 distinct features. Two types of feedback were applied to stimulate and motivate lifestyle changes. First, actionable health data were returned to participants via a web dashboard and interpreted by a study physician, starting from the second visit. Second, personal data-driven coaching was provided, including three face-to-face and six remote meetings, plus continuous email and phone support, starting from the third visit. Personal actionable possibilities were identified with the help of questionnaires, clinical laboratory tests and physical examination and focused on diet, exercise, mental wellbeing, stress and time management. Out of the 107 people enrolled, 96 completed the study. The data-driven coaching

92 positively impacted on the health of the participants, and 86% reported improvement in at least of the following aspects: diet, exercise, sleep, mental wellbeing, stress management, drinking or smoking
94 (Supplementary Figure 3). For example, the percentage of people who did not exercise decreased from 9% to 1%, the percentage of smokers decreased from 16% to 8%, and the percentage of daily
96 drinkers from 8% to 5%. A major achievement was the decrease in the prevalence of vitamin D deficiency (31% to 16%, Sallinen et al. The Journal of Nutrition, in press). The participants described
98 the wearable device, the return of personal health data and the tailored coaching as the most motivating aspects of the study (Supplementary Figure 3). Overall, the subjects were enthusiastic
100 about participating and 76% indicated that they would again participate in a similar study.

Longitudinal actionable changes

102 We defined a *phenotype* using the ensemble of questionnaires, anthropometrics, vitals and clinical laboratory tests. Actionable health issues were defined at baseline, including dyslipidaemia,
104 overweight and obesity, elevated systolic blood pressure, low vitamin D, elevated blood glucose, anaemia and self-reported obstructive sleep apnea (Supplementary table 1 and Supplementary Figure
106 4).

We first analysed the clinical measurements at baseline to define the group of individuals with Out-
108 Of-Range at Baseline (OORB) values. To explore if data feedback and coaching had a positive effect on objective health parameters, we modelled the longitudinal changes in the ORRB individuals, based
110 on the assumption that measurements outside the reference values represented an actionable finding to improve lifestyle and health. We analysed the average change per visit, adjusting for sex and age.
112 We found significant improvements (FDR<0.05) in several key health parameters for the OORB group during the course of the study, such as an increase in vitamin D levels and a decrease in blood
114 pressure, LDL-cholesterol, and total/HDL cholesterol ratio (Figure 2 and Supplementary Table 3).

Secondly, we obtained an overview of all the clinical variables and compared the individuals using
116 Principal Component Analysis (PCA). The first three PCs (Figure 2) accounted for 44.8% of the variance

and the major drivers of variability were cardiometabolic variables (for PC1 and PC3: BMI, insulin, fasting glucose, cholesterol, and lipoprotein profiles) and sex-dependent anthropometrics and haematological measurements (PC2). Trajectories for selected individuals showed the changes during subequent study visits and visualized the improvements in the clinical parameters (Figure 2 and Supplementary Figure 5).

In summary, we showed that the return of data as well as data-driven lifestyle coaching resulted in objective improvements of health behaviour and health outcomes, including physiological and laboratory measurements indicative of cardiovascular risk.

Multiomics signatures

Distinct sources of molecular variability

We next generated multiomics profiles and set out to explore the association of these variables with each other and with the clinical features. We first investigated the sources of variability in the omics, by partitioning the variance for each feature into personal variation (i.e. between-individual), known factors (age, sex and study visit) and residual unknown sources (for example biological, environmental or technical aspects). We found that the personal variation impacted all data types but to a different extent (Supplementary Figure 6). Autoantibodies represented a highly personal signature and on average 92% of the variance was explained by personal variation. Metabolites were dominated by personal variation (56-71% on average) but residual components were also present (23-35% on average). Proteins had similar average personal (49%) and residual components (45%). The microbiome data was dominated by unexplained factors (68% on average). These results were confirmed by an alternative distance-based method (Supplementary Figure 6). We observed that the average within-individual distance was lower than the between-individual distance, to a different extent for different omics, and autoantibodies showed the lowest within-individual distance, i.e. high similarity.

Understanding the molecular variability

142 We used Multi-Omics Factor Analysis (MOFA+)[11,12] to carry out an unsupervised analysis of the complete multiomics data, hence excluding the clinical variables and other phenotypic data. MOFA+
144 helped to integrate and interpret the measurements and their variability across all the omics layers. The analysis resulted in an interpretable low-dimensional representation in the form of a small number
146 of independent factors that captured the major sources of variability in the data and originated from simultaneous inclusion of baseline and longitudinal differences. The analysis facilitated the
148 identification of subgroups of samples and the molecular features that contributed to the ordination of the samples in the dimensions defined by the factors. An overview of the samples based on the learned
150 factors is given in Supplementary Figure 7. We identified 14 factors (F1-F14), each explaining a minimum of 2% of the variance in at least one data type. The fraction of the total variance explained
152 across the six omics types varied from 6% for gut microbiome to 95% for the autoantibodies (Figure 3). Some of the learned factors were predominantly associated with one omics type, while others
154 contributed to several omics, suggesting that the underlying biological determinants might affect different types of measurements simultaneously. We then explored the molecular basis of each factor.
156 First, we investigated the contribution of the original omics features, by inspecting the loadings on each factor, which represent their weights, in order to interpret the nature of the associated biological
158 domains. Second, we tested the association between the factors and the phenotype, including questionnaire data, clinical variables, fitness tests, activity and sleep data, and other metrics. Each
160 factor was linked to specific phenotypic characteristics (linear models, FDR<0.001, Figure 3 and Supplementary Table 4). Importantly, most of the factors were associated with distinct sets of variables
162 across the different categories and thereby defined molecular patterns that were linked to distinct aspects of lifestyle and health, including modifiable behavioural aspects, such as diet and exercise.
164 We then refined the top associations for each factor with a covariate-adjusted statistical model. We aimed at accounting for the correlation among observations from the same individual and fitted a linear
166 mixed model (LMM), with age and sex as fixed effects and the individual as a random effect. We also

interpreted the association in view of the contributing molecular features and pathways and the results
168 are presented below.

Obesity and insulin resistance. The top features with high positive loadings on F11 included
170 plasma proteins involved in pathways known to be dysregulated in obesity or dyslipidemia (LEP, IL-1ra (IL1RN), t-PA (PLAT), FABP4, FGF21, IL-6, LDL receptor)[13-18]. Interestingly, several proteins
172 reported as protective factors against obesity (GH1, IGFBP1, PON3)[19-21] had negative loadings. We found significant correlations between F11 and well-known metabolic traits and clinical measurements
174 (Figure 4 and Supplementary figure 9). These included positive association with BMI (p_{lmm}=1.53E−21), LDL-cholesterol levels (p_{lmm}=4.47E−03) and insulin resistance ($\log_{10}$HOMA-IR, p_{lmm}=6.51E−14). Also,
176 we found a negative association with HDL-cholesterol (p_{lmm} =2.16E-06) as well as with measures of physical activity and fitness gathered from the questionnaire, such as leisure-time exercise
178 (p_{lmm}=1.06E−03) and exercise habits (p_{lmm}=8.25E−04), or the activity levels in terms of steps/day measured by the wearable device (p_{lmm}=0.01). An inverse correlation was also observed with physical
180 fitness at the level of upper body (p_{lmm}=5.53E−05) abdominal (p_{lmm}=1.59E−03) and lower body (p_{lmm}=1.14E−03). Participants with first-degree relatives with diabetes had higher factor values
182 compared to the individuals who did not report family-history for diabetes (p_{lmm}=6.25E−03). Finally, an individual who was diagnosed with type 2 diabetes during the study had the highest factor values. We
184 therefore interpreted F11 as strongly related to obesity, insulin resistance and diabetes risk and pathogenesis as well as clearly associated with quantitative data on exercise and mobility. F11 was
186 also associated with overall health, as evidenced by a negative association with self-reported overall health (p_{lmm}=9.26E−07) and a positive correlation with coronary heart disease (CHD) risk score
188 (p_{lmm}=0.01). In summary, F11 assisted in estimating molecular patterns of health and behaviour that are associated with obesity as well as potential trajectories leading to diabetes.

190 **Impact of hormones and ethinyl estradiol.** F9 was influenced by sex and sex-specific biological differences in multiomics. In contrast, F14 was linked to the use hormone replacement therapy or
192 hormonal contraception in women. Young women reporting the use of a contraceptive containing

ethinyl estradiol (EE) had particularly high F14 values (p_{lmm}=2.28e−10). Consistent with this
194 observation, known estrogen-sensitive plasma proteins had the highest positive weights for F14 (Figure 4), but there were also contributions from cortisol and thyroxine levels, which we interpreted
196 as potential secondary effects[22,23]. Pulse (p_{lmm}=9.32E−03), hsCRP (log-transformed, p_{lmm}=7.40E−09) and leukocyte numbers (log-transformed, p_{lmm}=6.09e−05) also positively correlated with F14 and
198 alterations of these clinical variables were prominent in women with particularly high factor values. These observations indicated, in an unsupervised manner, that EE use is associated with strong
200 molecular and physiological effects on human biology, including increased levels of inflammation, impact on thyroid, cortisol levels and pulse. These effects are distinct from all the other sources of
202 variability in our study population,

Dietary habits. F3 and F6 were mostly influenced by metabolites and associated with distinct
204 dietary habits assessed with the questionnaire (Supplementary figure 10), such as consumption of fresh fruit and vegetables. However, when accounting for the effect of age, sex and individual, the
206 dietary characteristics were not significantly associated with the factors (p_{lmm}>0.05), suggesting that the associations may be explained by individual-specific (person-to-person) differences in dietary
208 patterns and not by changes in the diet during the study. Moreover, F7 was largely linked to caffeine use as determined both by the molecular nature of the features and the associations with questionnaire
210 data. Indeed, caffeine and its metabolites had the largest loadings for F7 (Figure 4), and this factor was strongly correlated with self-reported coffee consumption (p_{lmm}=7.63E−12).

212 **Lipids, free fatty acids and fatty acid esters.** F5, F8 and F12 (Supplementary figure 11) were each reflecting distinct aspects of the plasma lipid composition. Free fatty acids (FFA) contributed
214 mostly to F12, while fatty acid esters (FAEs), mostly in the form of acylcarnitines, contributed to F5 and F8. In the postabsorptive state, blood FFA are a result of lipolysis from adipose tissue and they
216 reflect dietary intake[24], while changes in the acylcarnitine pool can be linked to changes in fatty acid oxidation. Accumulation of acylcarnitines as products of incomplete mitochondrial fatty acid oxidation
218 has been associated with obesity and diabetes[25]. Even after adjusting for the covariates, F12 was

negatively associated with blood pressure (systolic, p=0.035; diastolic p=0.021), in line with the known
220 association between FFA and hypertension[26]. F5 and F8 were both strongly associated with clinical measurements indicating dyslipidemia, including total cholesterol (p_{lmm}=1.64E-08 and p_{lmm}=8.48E−10)
222 LDL cholesterol (p_{lmm}=7.13E-06 and p_{lmm}=1.74E−05), triglycerides (p_{lmm}=3.74E-05 and p_{lmm}=8.45E−7) and ApoB (p_{lmm}=3.24E-08 and p_{lmm}=9.11E−06), thus implicating dysregulation of lipid metabolism as
224 an underlying influence for F5 and F8 Importantly, F5 and F8 were only weakly associated with BMI (R2=0.004 and R2=0.006; p_{lmm}=0.05 and p_{lmm}=0.07), suggesting that these two factors were associated
226 with dyslipidemia independently of obesity.. Sex was a significant covariate for the associations seen for F5 (maximum p_{lmm}=1.21E-05) but not for F8 (minimum p_{lmm}=0.73).

228 **Hepatic function.** F2 was influenced by metabolites connected to liver function (Supplementary figure 12). Bile acids or their glycine or taurine conjugates had negative weights and a major impact in
230 the classification of the individuals along the F2 axis. Furthermore, F2 included liver-associated metabolites that on average were increased in the samples with negative factor values. These
232 metabolites are known to be increased after liver disease (biliverdin) or are known to be used to eliminate hepatic nitrogen pool (glutamine, hippuric acid, phenylacetylglutamine). The liver is a
234 fundamental organ in maintaining metabolic homeostasis, it modulates the composition of the blood metabolome and therefore we assumed that F2 reflected the structural and functional integrity of the
236 liver.

Autoantibodies. F1 was mostly explained by the presence of autoantibodies, it was influenced by
238 the binary nature of the autoantibody data (presence/absence) and by the stable autoantibody signature over time. Indeed, autoantibodies can be considered as an IgG reactivity barcode for each
240 individual[27]. F1 correlated well with the autoantibody counts and to a lesser extent with the age (Supplementary Figure 8), in agreement with the fact that autoreactivity is more common in the elderly,
242 possibly linked to age-associated B cells[28].

In summary, we demonstrated that we could dissect the overall pattern of molecular variation
244 between and within individuals using the multi-omics factor analysis. Each of the 14 factors reflected

distinct aspects of human biology, behaviour, lifestyle, use of drugs (hormones) or potential transitions to disease.

Correlation networks: linking molecular features with clinical variables, questionnaire data and digital health monitoring

We then performed correlation analysis, including all the multiomics data as well as an ensemble of quantitative or semi-quantitative measures consisting of clinical data, activity and sleep, fitness tests, and other scores. We computed a cross-correlation network between features of different types using two alternative metrics. For the between-individuals network (BIN), we averaged the measurements from all time points before calculating correlations. We also included 146 genetic trait scores obtained by summing up the contribution from all the variants associated with each trait as reported by the GWAS catalog. The within-individuals network (WIN) consisted of linear correlations of repeated measures of pairs of features within-participants. It estimated a common regression slope, representing a measure of association shared among individuals, and resulting from changes occurring at the individual level during the study. The BIN and WIN were calculated after age- and sex-adjustment and p-values were corrected for multiple hypothesis (FDR<0.05). We then identified distinct communities of interconnected features (modules), as an aid for interpretation.

Among the strongest correlations of the BIN ($|\rho| > 0.6$), we detected distinct measurements of the same molecular entity using different assays (i.e. TSH (clinical-PEA), $\rho = 0.96$; Cholesterol (clinical-GCMS) $\rho=0.82$), or associations between different features such as LDL-receptor protein and triglycerides ($\rho=0.82$), or LEP protein and BMI ($\rho=0.68$). The network consisted of 375 nodes and 570 edges (Supplementary table 5). Several clinical variables represented hubs with the largest number of associated connections to metabolites and proteins (Figure 5). These hubs were often inversely correlated with modifiable behavioural risk factors, such as wearable-based measures of physical activity (e.g. insulin with intense physical activities, waist circumference with number of steps). Similarly, measures of physical fitness (lower body, abdominal and upper body) correlated inversely with plasma LEP levels. Notably, the proteins with common genetic defects in familial

hypercholesterolemia appeared in the cardiometabolic subnetwork (LDLR, PCSK9, and ApoB). For
272 instance, PCSK9, a pharmacological target of LDL-lowering therapies, correlated positively to several glycerophospholipids and ApoB, but negatively to CMPF (3-Carboxy-4-methyl-5-propyl-2-
274 furanpropionic acid), a metabolite that is formed from the consumption of fish oil and may have positive metabolic effects[29]. The whole network included 24 GWAS summary scores (Supplementary figure
276 13), and 11 scores concerned haematological measurements (erythrocytes, leukocytes and thrombocytes). We observed a direct link between the genetic score and the corresponding trait
278 measured in this study, including haematological traits, but also associations between proteins or metabolites and the genetic susceptibility to a disease/trait with cardiometabolic relevance. For
280 example, we observed an inverse association between the genetic risk score for BMI in physically inactive individuals and several FAEs, carnitine and tyrosine. Furthermore, an inverse association was
282 observed between the genetic risk score for abdominal aortic aneurysm and IL-6RA levels, supporting the contribution of IL-6 signalling and inflammation in the pathogenesis of this disease[30]. These
284 observations indicate that the between-individuals variability may be explained at least partly by personal genetic differences and that these genetic differences exert their impact via specific
286 molecular pathways.

The WIN captured associations between pairs of features that resulted from concordant variation
288 in repeated measures obtained from the same individuals. This source of variation is assumed to be complementary to the BIN, it does not average or aggregate the data, neither does it violate the
290 assumption of independence of the observations. Thus, the edges in this network resulted from changes occurring over time and not due to baseline between-individuals characteristics. The network
292 consisted of 302 nodes and 611 edges (Supplementary table 5). Only 46 edges and 151 nodes were also detected in the BIN, reflecting how BIN and WIN highlight non-overlapping correlations, i.e. they
294 reveal distinct types of biological associations. For example, in an inflammation-related subnetwork (Figure 5), hsCRP and leukocytes lay in the proximity of cytokines, cytokine receptors, proteins
296 involved in leukocyte functions and members of the tryptophan metabolic pathway (kyneurine and indoles). This subnetwork was not revealed in the BIN and the observed edges likely originate from

298 individuals transitioning through inflammatory states or infections during the study, although other sources of variations (season, exercise etc.) cannot be excluded. Other edges specifically observed in
300 the WIN showed metrics of activities and sleep in the proximity of several metabolites and proteins. Among the proteins, we observed well-known members of lipid metabolism pathways (LEP, LPL) and
302 proteins with related functions (PTX3[31,32], NRP1[33], PRSS8[34]). Correspondingly, FFA and FAEs appeared in this subnetwork. These correlations suggest that changes in dietary factors, fat metabolism, physical
304 activity and sleep behavior as a result of the lifestyle coaching could be further investigated as possible explanations for the observed effects.

306 ***Personal trajectories***

In order to stimulate lifestyle changes and improve health, we defined personalized, actionable
308 data-driven possibilities for lifestyle guidance for each participant. This strategy resulted in subgroups where similar changes in actionable clinical variables were present. When considered at the level of
310 individuals, the changes unfolded into personal trajectories, and often a connection with the patterns in multiomics data were established. Changes in diet and exercise were common among participants,
312 as illustrated by the case of a 28-year male, where the tailored lifestyle change (nutrition and exercise) resulted in an improvement of clinical variables and self-rated health (Figure 2 and Figure 6). At
314 baseline, he presented with obesity, high systolic blood pressure, dyslipidaemia, elevated insulin levels and elevated hsCRP (Figure 6A). During the study, he reported increases in self-rated health, frequency
316 and amount of exercise (Figure 6C). The latter was also objectively confirmed by the activity levels detected by the wearable device (Figure 6B). The sustained level of activity resulted in longitudinal
318 changes in key actionable clinical variables at the end of the study (Figure 6A), including decreased BMI, improved lipid profile, reduced low-grade systemic inflammation, reduced systolic blood
320 pressure, normalization of insulin levels and improvement of the estimated insulin resistance. These interpretable changes reflected in molecular changes, as shown by the MOFA+ factors (Figure 6D).
322 Indeed, the improvement in BMI, lipid profile and insulin resistance, combined with an increase in physical activity, was reflected as a decrease in F11 values. We observed decrease of obesity- and

inflammation-associated proteins and other adaptations suggesting an involvement of the GH/IGF-1 axis. Similarly, the changes in F8 and F10 - associated with fatty acid esters and lipid metabolism - reflected the variation in the total cholesterol levels. Several acylcarnitines peaked at the third visit, suggesting a metabolic adjustment during a transition period toward increased physical activity. For comparison, we show (Figure 2 and Supplementary figure 14) the case of a 36-year-old female, presenting with obesity, dyslipidaemia, hyperinsulinemia and hyperglycaemia at baseline. The study protocol required a referral to a physician, and she was indeed diagnosed with type 2 diabetes. During the study, phenotypic changes occurred: reduction in the glucose, insulin and cholesterol levels, as a result of a new therapeutic intervention (Metformin, Atorvastatin, Empagliflozin), while she did not undertake a genuine lifestyle change and did not increase physical activity. Interestingly, the F11 levels did not change much, this individual remained an outlier at all the time points and we did not observe a trend in the corresponding molecular features indicating reduction of inflammation and adiposity.

A case of a participant with a respiratory tract infection is illustrated in Supplementary Figure 15, it shows the dysregulation of metabolic pathways during infection as previously observed[1,6], and highlights how metabolic signatures can be prominently altered during infections.

340 ## *Discussion*

The convergence of systems medicine, digital health, big data, consumer-driven healthcare and
342 social networks is at the heart of the P4 healthcare. To facilitate the adaptation of the P4 approach into the current healthcare systems, longitudinal health intervention studies are needed. Indeed,
344 numerous initiatives exist to profile healthy and diseased individuals with clinical features, multiomics and digital health monitoring[1-8]. However, fewer studies have simultaneously combined longitudinal
346 multiomics profiles, digital health data monitoring, data feedback and tailored lifestyle coaching. Here, we report a truly comprehensive approach to generate longitudinal data from 96 people who
348 underwent tailored lifestyle coaching for over 16 months. Our study provides several steps to promote an understanding of human biology and health over time and, at the same time, a data-driven,
350 individualized approach to motivate and monitor the impact of lifestyle changes. Firstly, our data emphasize the importance of multiomics profiles in preventive and personalized medicine approaches.
352 Most of the published large-scale medical research initiatives have explored predominantly the impact of genetics on health parameters. We think that the precision medicine toolbox should include
354 multiomics and digital health readouts, longitudinal measurements for each individual. Secondly, we have shown that by integrating all the data in an unsupervised analysis we can rediscover known
356 associations between molecular features and lifestyle changes, health behaviours, adiposity, diet, physical activity or hormonal use as well as identify numerous novel associations. We have also shown
358 how data from a wearable device correlate with changes in specific molecular pathways, which could help to understand the molecular effects of e.g. exercise and sleep on specific aspects of human
360 biology. Thirdly, our data-driven feedback and individualized lifestyle coaching stimulated behavioural changes and we anticipate that this model could become broadly applicable in the future. In this study,
362 genetics, questionnaire and clinical measurements were returned to the participants in real-time, while the full multiomics data were analyzed retrospectively. The analysis of all molecular data at the end of
364 the study also helped to ensure lower cost, higher quality and consistency, and elimination of batch effects.

366 Our data analysis resulted in a low-dimensional space to explore the complexity of the multiomics and the connection to known sources of variation. Among those, sex, age and BMI are among the
368 most studied and often are confounders in association studies. For this reason, we regressed out the effect of age and sex in the correlation networks, but we allowed the effect of these covariates to
370 appear in the MOFA+ analysis, in order to verify if separate, independent axes of variability could be retrieved. Indeed, we verified that BMI, as a proxy for adiposity and obesity, could only be strongly
372 associated with one factor (F11) and that there was no strong significant association of obesity with any of the other factors. Similarly, sex was associated only with a few factors (F5, F9, F11). Therefore,
374 the identified axes of variation represented a spectrum of molecular variation that could be attributed to a variety of lifestyle factors and could not simply be explained by the confounding effects of obesity,
376 age or sex. This strongly supports the power of our analysis to extract independent axes of molecular variability of potential etiological and pathogenetic importance, and hence with opportunities for
378 unbiased health monitoring.

An example of a highly interesting and novel observation is that the use of oral contraceptives
380 containing EE in a subset of the female participants was alone sufficient to influence the covariance of the proteome and metabolome. The effect was so distinct that F14, as uncovered from this
382 unsupervised MOFA analysis, was almost completely due to the use of this one hormonal drug. We suggest that the strength of this association could have been even greater if we had detailed
384 information on the days of the administration of the hormone and the days of the menstrual cycle of all females when samples were obtained. These effects were identified in a data-driven manner and
386 represented a distinct dimension of variability in human biology influenced by an external hormone. Thus, the hormonal effects were strong enough to be picked up above all other causes of variability
388 and noise. F14 could therefore be a potentially useful biomarker to assess exposure to EE as well as associated health effects. The association with pulse and the effects on inflammation, adrenal and
390 thyroid function have been individually investigated before[22,23], but the full depth and width of this signature have not been previously described. EE is a strong synthetic hormone and hence it is not as
392 unexpected that modulation of this pathway could have consequences on the proteome and

metabolome as well as body physiology. However, considering that the use of this contraceptive is
394 common, we point out that this will need to be accounted for as a potential bias in all epidemiological
and multiomics studies. The EE-inducible signature could otherwise cause strong false interpretations
396 in biomarker studies. For example, serum TFF3 has been reported to be elevated in women with breast
cancer[36] and FETUB is a highly abundant liver-secreted protein sensitive to estrogen and is reported
398 to be increased in type 2 diabetes[37,38].

Our analysis showed that genetic determinants could explain part of the variability in the
400 multiomics features. This raises the question of whether this type of multi-omics data integration and
unsupervised analysis could help to dissect the molecular effects mediating the mechanisms and
402 pathways on how genetics may influence disease onset. Several hints of such observations were seen,
such as the associations of IL-6 receptor signalling and abdominal aortic aneurysm.

404 We acknowledge some limitations of this study. Firstly, the sample size may limit the discovery of
weak associations and hence the conclusions should be confirmed in larger cohorts. Nevertheless,
406 we retrieved several known associations, likely resulting from strong underlying effect sizes. For
example, we showed that several blood cell measures in our study were under genetic control, in
408 agreement with the high heritability of haematological traits[41]. By extension, it is possible that the
associations with cardiometabolic relevance observed in our study also have larger true effect sizes.
410 For example, it was remarkable how key cardiovascular risk genes and drug targets, such as PCSK9
strongly clustered in the network analysis. It has been previously observed that a longitudinal study
412 design substantially increases the power to identify molecular changes in comparison to a groupwise
analysis in a population of similar size[4]. Therefore, the presented resource and data analysis could
414 reveal several other relevant interrelationships to be explored further and validated in external data
sets. Our work was not a formal interventional study but included longitudinal observations of people
416 undertaking a tailored health intervention. Individual trajectories and multiomics profiles highlighted
specific connections when specific cases or subgroups were considered. In addition, in a longitudinal
418 observational study, changes over time may also be caused by other unknown parameters, such as

seasonal variability known to impact on immune systems gene expression and cellular
420 composition[42,43].

Our study illustrated a person-centric data-driven health monitoring that could become part of the
422 future health care practice. This involved integration of clinical, genetic, multi-omics and digital health data as well as unbiased monitoring of longitudinal trends. This study demonstrates the power of
424 combining multi-omics and lifestyle data as well as new opportunities for predicting health trajectories in a holistic, unbiased data-driven manned. This could lead to a re-definition and refinement of the
426 traditional disease-based taxonomy as well as definition of specific transitions between health and disease. This could contribute to preventive approaches via lifestyle and behavioural changes or
428 pharmaceutical interventions.

Acknowledgements

430 We thank all the study subjects for their generous participation and commitment. We express our sincerest thanks to Riina Aaltonen, Annette Evokari, Iiro Hietamäki, Anna Seppänen and Paula
432 Vartiainen for their expert assistance. The DHR program was coordinated and managed by the Center for Health and Technology, University of Oulu, Finland. Genotyping was performed by the Institute for
434 Molecular Medicine Finland (FIMM) Technology Centre, HiLIFE, University of Helsinki, Finland.

Author contributions

436 F.M, T.J., R.S. and O.K. wrote the paper with contributions from all the authors. F.M. designed and performed the bioinformatics analyses, interpreted the results, prepared the figures and wrote the
438 primary version of the paper. T.J. performed bioinformatic data analysis and interpreted the results. R.S. coordinated the data collection, supervised the experiments, and was responsible for the project
440 management. R.S and O.K. designed the project, with contributions from H.V., H.H. and M.P.H., and provided conceptual advice and support. M.P.H. acted as a coordinator of the DHR consortium. H.S.

442 and Thonas Moritz performed the metabolomics experiments, analysed the data and contributed to the interpretation of the results. F.B. and L.E. performed the microbiome experiments, analysed the
444 data and contributed to the interpretation of the results. C.H., M.N., and P.N performed the autoantibody experiments, analysed the data and contributed to the interpretation of the results. E.W.
446 and S.R. provided the KardioKompassi algorithm. R.M., T.P., M.B. and Timo Miettinen were responsible for data management, database administration, health dashboard and software
448 development. H.L. was the study physician. P.H. performed genotype imputation. Anu Karhu, I.J., K.K., H.V., H.H., Antti Kallonen, M.E., H.S. and M.L. conducted research.

450 *Competing interests*

O.K. received research funding from Vinnova for collaboration between Astra-Zeneca, Takeda,
452 Pelago, and Labcyte. O.K. is also a board member and a co-founder of Medisapiens and Sartar Therapeutics, and has received a royalty on patents licensed by Vysis-Abbot. R.S. is currently
454 employed at Crown CRO.

456 ## *Methods*

Ethical permit and consent

458 The study was conducted in line with the Declaration of Helsinki and approved by the Coordinating Ethics Committee of the Helsinki University Hospital, Finland. Each participant provided informed 460 written consent for the study, biobanking of samples, publication and data sharing. Participants were free to drop out any time, but their samples and data were still available for analyses. If a participant 462 withdrew the consent, samples and data were discarded.

Overview

464 The observational cohort study was conducted at the Institute for Molecular Medicine Finland (FIMM), HiLIFE, University of Helsinki, Finland, between September 2015 and January 2017. 466 Recruitment was performed in September 2015, and five study visits followed, approximately every four months, (Supplementary Figure 1). Every visit included a health check-up and blood and urine 468 sampling. Before or after every visit, participants collected fecal and saliva samples, filled out a questionnaire, and performed fitness tests. Data on physical activity and sleep was collected from the 470 second visit onward with an activity watch. Key actionable health data were returned to the participants via a web dashboard starting at the second visit. Tailored health and wellness advice and 472 coaching was provided by two personal trainers from the third visit onward. Between visits 4 and 5, participants could compare their data to summary measures calculated with the other participants' 474 data.

Eligibility criteria and recruitment

476 The requirements included: age of 25-64 years at the study start, sufficient computer skills and Internet access via a smartphone compatible with the provided smartwatch; sufficient English 478 language knowledge to be able to understand simple messages and to use health and wellness

applications. We excluded individuals with severe diseases (cancer, cardiovascular, debilitating
480 neurological, psychiatric or orthopaedic diseases). However, individuals with risk factors for chronic diseases (e.g., obesity, elevated blood pressure, dyslipidaemias, disturbances in sugar metabolism,
482 mild forms of metabolic syndrome, smoking, moderate drinking or sleep problems) were allowed. Individuals diagnosed with or suspected of having rare monogenic diseases were excluded. In
484 addition, individuals under custody, with special needs or with limited decisional capacity were excluded, as well as people suffering from severe forms of alcoholism and depression. Pregnant
486 women were excluded and women becoming pregnant during the study were no longer asked to provide samples or contribute to the study. Altogether, 645 clients of a private occupational health
488 service (Mehiläinen Töölö, Helsinki, Finland) were invited to participate (Supplementary Figure 1). People interested in participating (n=125) filled out a questionnaire to assess eligibility. A total of 107
490 volunteers of European descent from the Helsinki metropolitan area were selected to participate and 96 completed the study (Supplementary Table 1).

492 ***Return of personal health data***

The ensemble of anthropometrics, clinical laboratory tests, and physiological measurements is
494 called clinical variables in this paper. We returned actionable health data via the Health Dashboard web application, which allowed participants to: explore and compare their data against reference
496 values and the mean values for the other participants, fill out questionnaires and read informational material. The clinical variables and their reference values were returned starting at visit 2. A physician
498 interpreted the clinical data and was available to discuss the results with the participants. The occupational health service communicated any medically relevant finding requiring immediate actions,
500 while the study group communicated non-acute findings. Clinical decisions were made according to the national Current Care Guidelines (https://www.kaypahoito.fi/). Genetic data were returned to
502 participants under the guidance of a clinical geneticist after visit 2. A personal 10-year risk for coronary heart disease (CHD) was communicated using KardioKompassi[44]. The risk model is based on both
504 traditional (sex, age, family history, smoking, systolic blood pressure, total and HDL cholesterol) and

hereditary risk factors (approximately 49,000 SNPs). If the risk was >10% the participant was referred
506 to a doctor. We also communicated the risk for low serum 25(OH)D concentration after visit 4 (Sallinen et al., The Journal of Nutrition, in press). We returned visualizations of questionnaire data on diet,
508 physical activity, sitting, sleeping, subjective health status, and mental wellbeing after visit 4. We also determined a self-reported obstructive sleep apnea risk score[45]. Participants were able to monitor their
510 physical activity and sleep data using the Withings Health Mate app starting at visit 2.

Coaching and group meetings

512 Two personal trainers (PTs) coached participants from visit 3 onward. Coaching included nine 30-minute private meetings (three face-to-face and six remote), email/phone support, as well as group
514 meetings. The PTs were accredited by the European Health and Fitness Association. No structured, evidence-based coaching protocol was used, but personal actionable possibilities were defined to
516 help participants change their behaviour and improve their health. With the help of a physician and a nutritionist, the PTs translated and customized actionable possibilities to specific recommendations.
518 The PTs had access to participants' age, clinical variables, fitness test data, and information about their occupation, exercise, and diet. Tailored health advice and coaching were based on each
520 participant's behaviour, health risks, lifestyle, and goals. One to three relevant, personalized and actionable opportunities were offered to guide and motivate participants to make lifestyle changes to
522 optimize wellness and health and delay predicted pathologies. Personalized advice usually focused on diet, exercise, mental wellbeing, or stress and time management. If necessary, a physician limited
524 exercise. Twenty-one informational group meetings were organized during the study, where participants could interact with a physician, a nutritionist, a nurse, PTs, and other experts. Participation
526 in these meetings was voluntary except for the first, during which a physician and a geneticist interpreted the clinical variables data as well as the CHD risk prediction.

528

530 ***Experimental procedures***

Health check-up and clinical variables

532 Health check-ups occurred on weekdays between 7:30 and noon. Body weight, height, waist and hip circumferences, blood pressure, and pulse were measured using standard procedures. 534 Participants were asked about medications, dietary supplements, and the use of health care services. Blood and urine samples were collected at every visit. Fasting (≥8 h) blood samples were collected, 536 and clinical chemistry assays were performed on blood, plasma or serum, at the diagnostic laboratory of Mehiläinen Töölö (Helsinki, Finland), United Medix Laboratories Ltd (Helsinki, Finland) and HUS 538 Diagnostic Center (Helsinki, Finland). Urine samples (≥2 h without urinating) were collected using standard procedures. A dipstick test was performed on the urine samples at the diagnostic laboratory 540 of Mehiläinen Töölö (Helsinki, Finland). Aliquots of blood, plasma, serum and urine were frozen at -20°C and stored in liquid nitrogen for biobanking.

542 ***Questionnaire***

Before every visit, participants filled out an online questionnaire, including approximately 150-190 544 questions, depending on the visit, and covering the following: personal information; sociodemographic and socioeconomic characteristics; familial and individual disease history; functional capacity and 546 health; mental wellbeing; physical activity and exercise habits; diet (including food frequency questionnaire, FFQ); smoking; alcohol consumption; sleep; occupational health; personality traits; 548 attitudes and expectations towards lifestyle changes; monitoring own health and wellbeing; expectations towards health technology. Healthy Food Intake Index is a food-based diet quality index, 550 calculated from the FFQ data and adapting an available method[46].

552

Fitness tests

554 After every visit, participants were instructed to perform lower-body (squats, repetitions/30s), abdominal (sit-ups, repetitions/30s) and upper-body (push-ups, max number of repetitions) muscular
556 fitness, balance and mobility tests. Participants executed the tests and uploaded the results to the Health Dashboard.

558 ### *Activity and sleep monitoring*

After the second visit, participants were equipped with the Withings Activité Pop smartwatch,
560 connected to the Withings Health Mate app, to measure physical activity, energy expenditure and sleep. Participants were requested to wear the watch until the end of the study. Wellness Warehouse
562 Engine[47] embedded in the Health Dashboard was used to authorize and provide the research group access to participants' data. Only aggregated daily activity and sleep data were exported and included
564 in this study.

Salivary cortisol

566 Participants collected saliva samples within two weeks of every visit, using Cortisol-Salivette® with a synthetic swab (Sarstedt). Four samples (awakening, 15 min and 30 min after wake up, bedtime)
568 were collected on a typical weekday. Time and mood at sampling were recorded. Samples were stored at +4°C until aliquoting and storage at -20°C. Salivary cortisol levels were determined at the University
570 of Trier (Trier, Germany) using a DELFIA immunoassay[48]. The stress scores derived from the measurements included: AUCi, AUCg (according to[49]), awakening, evening, peak and Delta (peak -
572 ground) cortisol levels.

DNA extraction and genotyping

574 DNA was extracted from whole blood with Chemagic MSM1 (PerkinElmer). Genotyping was performed at the FIMM Technology Centre (HiLIFE, University of Helsinki, Finland) using

576 InfiniumCoreExome-24 v1.0 DNA Analysis Kit, iScan system and standard reagent and protocols (Illumina). Genotypes were pre-phased with ShapeIT2 and imputed with IMPUTE2. Two pre-phased
578 reference panels were used (--merge_ref_panels): 1000G Phase 1 and a Finnish low-coverage WGS imputation reference panel, composed of 1,941 whole-genome sequences (SISu project). Imputation
580 resulted in 30.3 million quality-filtered variants (R^2>0.3 and missingness<0.05).

GCMS and LCMS

582 GCMS and LCMS experiments were performed at the Swedish Metabolomics Center (Umeå). 100 µl of plasma were processed as described[50], with the following details: extraction with 900 µl of 90%
584 v/v methanol, containing internal standards for both GCMS and LCMS, at 30 Hz for 2 minutes; protein precipitation at +4 °C; centrifugation at +4 °C, 14 000 rpm, 10 minutes. 50 or 200 µl of supernatant
586 were evaporated to dryness in a speed-vac concentrator, for GCMS or LCMS analysis respectively, and stored at -80 °C. Quality control (QC) samples were created by pooling supernatants. MSMS
588 analysis (LCMS) was run on the QC samples for identification purposes. Sample batches were created according to a randomized run order. For GCMS, derivatization and analysis were performed as
590 described previously[50], with the following modifications: 0.5 µL of derivatized sample; splitless injection with a L-PAL3 autosampler (CTC Analytics AG); 7890B gas chromatograph (Agilent Technologies);
592 chemically bonded 0.18 µm Rxi-5 Sil MS stationary phase (Restek Corporation); column temperature increased from 70 to to 320 °C at 40 °C/min; Pegasus BT TOFMS (Leco Corporation); solvent delay of
594 150 s; detector voltage 1800-2300 V. Unprocessed MS-files were exported from the ChromaTOF software in NetCDF format to MATLAB R2016a (Mathworks), where processing occurred, including
596 baseline correction, chromatogram alignment, data compression and Multivariate Curve Resolution. The extracted mass spectra were identified by comparisons of their retention index and mass spectra
598 with known libraries using the NIST MS 2.0 software[51]. Annotation was based on reverse and forward searches in the library. LCMS experiments were performed as described[52] and all data processing was
600 performed using the Masshunter Profinder version B.08.00 (Agilent Technologies). The processing was performed both in a target and an untargeted fashion. For target processing, a predefined list of

602 metabolites commonly found in plasma and serum were searched for using the Batch Targeted feature extraction in Masshunter Profinder. An-in-house LCMS library, built up by authentic standards run on
604 the same system with the same chromatographic and MS settings, was used for the targeted processing. The identification of the metabolites was based on MS, MSMS and retention time
606 information.

Autoantibody bead arrays

608 Autoantibody profiling on antigen bead arrays was performed as previously described[27], at the Autoimmunity and Serology Profiling facility at SciLifeLab (Stockholm).

610 ### *PEA*

Plasma proteins were quantified using Proximity Extension Assay (PEA) at Olink Bioscience
612 (Uppsala), using 6 panels: Cardiometabolic, CVD II, CVD III, Inflammation I, Metabolism and Oncology II. Each panel assayed 92 proteins using a matched pair of antibodies coupled to oligonucleotides,
614 which form an amplicon by proximity extension and can be quantified by real-time PCR. The data were normalized against an extension control and an interplate control and expressed as Normalized Protein
616 eXpression (NPX) values, which represent an arbitrary relative quantification unit on log2 scale. The NPX values below the limit of detection (LOD) were considered missing and their value was replaced
618 with the LOD value for each assay.

Microbiome analysis

620 Participants collected faecal samples within two weeks of every visit. Samples were collected in precooled vials placed in styrofoam boxes with ice gel packs and then stored at +4°C for a maximum
622 of one day until aliquoting, freezing at -20°C, and storage in liquid nitrogen without additives. Thawed faecal samples were spun-down and DNA was extracted, with 50 ng of DNA submitted to PCR
624 amplification as described[53], using 341f and 805r primers (CCTACGGGNGGCWGCAG and

GTGBCAGCMGCCGCGGTAA) for the V3–V4 regions of 16S rRNA[54]. Sequencing was done on an
626 Illumina MiSeq with 2x250 bp reads. After quality trimming with Cutadapt, an ASV (amplified sequence variants) table was generated using the DADA2 pipeline[55], including the following steps: filtering and
628 trimming, learning of error rates, dereplication, sample inference, read pairs merging, removal of chimeras and taxonomy assignment using SILVA v128 database.

630 ***Bioinformatic analyses***

Longitudinal analysis

632 We applied Generalized Estimating Equations (GEE) to the quantitative clinical variables to investigate the longitudinal changes while controlling for sex and age. As data feedback and coaching
634 started respectively from visit two and three, we excluded the first visit and considered the second visit as baseline. Four time points (0-4) were then considered and we aimed at extracting the average
636 change per visit, assuming the same change in the values between any two successive visits. Furthermore, for each variable, individuals were classified as Out-Of-Range at Baseline (OORB) if the
638 values were outside the reference range (Supplementary Table 2) at baseline. We assumed that the longitudinal changes could be distinct for individuals classified as ORRB. In other words, we allowed
640 the effect of coaching and data feedback to be different in the two groups by introducing an interaction term. If the OORB group included at least five individuals, then the variable was modelled as:

642 value ~ Sex + Age + Time.point + OORB + Time.point:OORB

Otherwise, a model with no groups of individuals was considered:

644 value ~ Sex + Age + Time.point

GEE models were fitted using the geepack library and exchangeable correlation structure. We
646 extracted the effects, their standard errors and p-values using the `esticon` function in the doBy library. If no interaction was specified, the coefficient for Time.point represented the estimated change

648 for all the individuals, expressed as the change occurring between two successive visits. If the interaction was included, we considered the change occurring in the ORRB group between two
650 successive visits, and we extracted the effect as the linear combination of the coefficients of Time.point and OORB. P-values were adjusted with the Benjamini-Hochberg method. Model
652 prediction of the variable values was visualized by stratifying for sex and OORB group. The 95% confidence levels were estimated by bootstrapping with 1000 replications.

654 ***Dimensionality reduction***

We selected the quantitative clinical variables and imputed missing values using the `imputePCA`
656 function in the missMDA package. Principal Component Analysis (PCA) was performed with the `PCA` function in the FactoMineR package on scaled data. Variable contribution to a given PC was defined
658 as the ratio between the squared cosine of a variable and the sum of the squared cosines for all the variables for that component.

660 ***Data preprocessing***

Activity and sleep. We obtained summary measures for the activity and sleep data by calculating
662 average values for the different variables in the previous 30 days before each visit. We considered only samples for which at least 10 days were included in the calculation.

664 *GCMS.* The relative quantities (RQs) were log2-transformed and missing values were imputed with the KNN algorithm. Data were normalized using the RUV4 method in the ruv R library[56]. `RUV4` was
666 applied to remove sources of technical variability, including batch effect and the signal drift over time. Briefly, we used the internal standards (IS) as negative controls, k=4 and a design matrix with
668 individuals and visits as covariates, in order to estimate the matrix W of unwanted factors and their respective α coefficients. The number of factors to remove (k) was chosen with the `getK` routine, but
670 was ensured not to exceed 1/3 of the number of the IS. The normalized relative concentrations were obtained by subtracting the effect of the W components from the RQs. The IS values were inspected

672 before and after normalization to ensure a removal of the signal drift over time and a reduction of the Coefficient of Variation (CV). Estimation of the Intraclass Correlation Coefficient (ICC) and PCA plots
674 were also evaluated to inspect the performance of the normalization method.

LCMS. The negative and positive modes from LCMS experiments were processed separately.
676 Unidentified metabolite peaks and metabolites with more than 25% of missing data were removed. RQs were log2-transformed and missing values were imputed with KNN. `RUV4` adjustment and
678 inspection of the results were performed as described above with k=2 or k=1 for LCMS-neg and LCMS-pos data, respectively.

680 *Autoantibodies.* We considered: continuous Median Fluorescence Intensity (MFI), discrete binned and binary (0=undetected, 1=detected) data (see [27]). MFI values were normalized with the Probabilistic
682 Quotient Normalization[57], with a median reference profile, and then log2-transformed.

16S rRNAseq. The ASV count table represents an analogue of the traditional Operational
684 Taxonomic Unit table. We inspected the taxa prevalence (the number of samples in which a taxon has nonzero counts) and the total abundance (sum of the counts in all samples) and the abundance
686 distribution. Using phyloseq R library, we agglomerated the counts to the genus level, to reduce functional redundancy. The genus-level data were filtered to remove taxa with missing phylum
688 annotation, prevalence ≤2 and total abundance ≤10. We inspected the ordination of the samples using several distance metrics. We then converted the genus-level count to a DESeq2 dataset and used the
690 Variance Stabilizing Transformation (VST), which normalizes with respect to the library size and gives a matrix of approximately homoscedastic values that can be used for downstream analyses. As a
692 major source of batch effect was represented by the experimental plate, we verified that the VST conversion also reduced the library size effect by visualizing the sample ordination, using MDS with
694 Bray-Curtis distance for the genus-level counts and Euclidean distance for the VST values. We also formally tested the reduction of the batch effect, by looking at the association between the first two
696 axes of the sample ordination plots with the plate ID. The estimation of the α-diversity for each sample was done using the original unfiltered counts.

698 ***Integration of multiomics experiments***

A MultiAssayExperiment object was assembled with all the continuous clinical and omics data, 700 namely RUV4-nomalized data for GCMS, LCMS-neg and LCMS-pos, log2MFI for autoantibodies, NPX values for PEA assays and VST-transformed values for 16S counts. Data filtering to remove unwanted 702 features included: removal of internal standards from GCMS and LCMS; removal of proteins NPX values < LOD (i.e. missing data) in more than 25% of the samples; removal of FS, CCL22 and BDNF 704 (technical issues, Olink communication); removal of autoantibodies with background fluorescence in all samples (scored reactivity values ≤0.5); removal of bacterial taxa with a prevalence ≤30%. We used 706 the filtered object for all the downstream analyses. The resulting dataset included 136 GCMS metabolites, 104 LCMS-neg metabolites, 163 LCMS-pos metabolites, 174 autoantibodies, 501 708 proteins and 85 bacterial taxa (Supplementary table 2).

Variance partition analysis

710 For each omics type, between- and within-individual variation was inspected with a distance-based method and with variance partitioning analysis. For the distance method, Euclidean distance 712 between all pairs of samples was calculated. Then, the within-individual distance was calculated as the median value of the distance values of the sample pairs from the same individual. This value was 714 plotted together with the distribution of the remaining distance values, i.e. the distances between one individual and the rest of the individuals. For the variance partitioning method, a linear mixed model 716 was fitted with lme4 R library, independently to each feature with nonzero variance. We included the individual as a random intercept and age, sex and time point (0-4) as fixed effects. The fixed effect 718 variance, random intercept variance and residual variance components were extracted, and the relative fraction calculated. The random intercept variance represented the between-individual 720 variance, while we interpreted the residual variance as the within-individual variance not accounted by the fixed effects.

722

Multi-Omics Factor Analysis

724 Multi-Omics Factor Analysis v2 (MOFA+) provides a set of factors that capture biological and technical sources of variability[11,12]. It infers the axes of heterogeneity that are shared across multiple
726 modalities and those specific to individual data modalities. We used the "intercept_factor" branch of the code repository (https://github.com/bioFAM/MOFA2/tree/intercept_factor). For training, we
728 selected the samples that had a measurement in all the omics layers (n=359). We considered a Gaussian likelihood for the continuous measurements for all the layers, except for autoantibodies,
730 which were considered in their binary form (0=undetected, 1=detected) with Bernoulli likelihood. Data were not scaled. We trained 10 alternative models in Python with a random seed, starting from 20
732 factors and the following options: iter="10000", convergence_mode="medium", dropR2="0.02". The model with the best value of the Evidence Lower Bound (ELBO) was selected. We checked the
734 robustness of the learned factors by inspecting the Pearson correlation between the factors obtained by all the runs (Supplementary Figure 6). We then computed the fraction of the total variance explained
736 by each factor and the fraction of variance explained by each factor in each layer. We inspected the factor loadings to understand the contribution of the original features. A feature with a higher absolute
738 loading has a higher weight on the factor, but because the loadings are not directly comparable, their scaled values were used for visualization. The sign of the loading defines a direct (positive) or inverse
740 (negative) proportionality with the corresponding factor, and features with similar loadings contribute similarly to the factor. We inspected the factor values and to visualize and cluster the samples on the
742 reduced space.

Association between factors and phenotypic variables

744 In order to test the association between the MOFA+ factors and the sample characteristics, we gathered a collection of phenotypic information including: clinical variables; questionnaire data (family
746 history, exercise and physical activity, functional capacity and health, mental health, diet, smoking, alcohol use and sleep habits); Healthy Food Intake Index; KardioKompassi risk; sleep apnea score;

748 stress scores; fitness tests; sleep and activity summaries from the wearables. For each combination of factor and phenotypic variables, we fitted a linear model with the factor values as outcome and the
750 phenotypic variable as predictor. Reported R^2 values were derived from these models. For the categorical variables, the predictor was considered an ordered factor if the factor levels corresponded
752 to ordered levels and the variable could be considered as a qualitative or semi-quantitative ordinal variable. A False Discovery Rate (FDR) was calculated using the Benjamini-Hochberg method. The
754 candidate associations for further screening were obtained at FDR<0.05, while the associations reported in Figure 3 satisfy a FDR<0.001 threshold, in order to better control for false positives arising
756 from the multiple hypotheses tested. The selected associations were refined with linear mixed models as implemented in lme4 library. We modelled the LF values with the individual as a random intercept
758 and age and sex as fixed effect. We refer to these models as the covariate-adjusted models. P-values for these models were obtained with the "Type II ANOVA" as implemented in the `Anova` function in
760 the car library, with a Kenward-Roger F test.

Population stratification

762 The DHR and the 1000 Genome phase 3 genotypes were merged. Analyses were done with PLINK v1.9. Only autosomal biallelic SNPs with genotyping rate >95% and MAF>5%. were considered. A set
764 SNPs in approximate Linkage Disequilibrium was obtained with the option --indep-pairwise 50 5 0.2 and PCA was performed. To predict the ethnicity, a Linear Discriminant Analysis model (`lda` in MASS)
766 was trained in R with the PCA scores of the 1000 Genomes only and tested on the DHR samples.

GWAS summary scores

768 We considered 146 traits from the GWAS catalog v1.0.1 (https://www.ebi.ac.uk/gwas/) for selected ontology categories: body measurement, cardiovascular disease, cardiovascular
770 measurement, hematological measurement, inflammatory measurement, lipid or lipoprotein measurement, liver enzyme measurement, metabolic disorder and other (fasting blood glucose,
772 vitamin D levels and thyroid stimulating hormone). For each trait, only the studies meeting the following

criteria were considered: at least one SNP with p-value<1E-08, sample size >5000, at least 10 SNPs
774 reported. The study with the largest sample size was considered for the traits with multiple associated studies. For each biallelic SNPs, the reported effect size of the risk allele was considered as a weight.
776 Summary scores were computed by multiplying the imputed genotype dosage of each risk allele times its respective weight and summing across all SNPs.

778 ***Between- and within-individual cross correlation network***

We considered the continuous measurements for all the omics layers, together with a collection
780 of measurements including: GWAS summary scores; gut microbiome alpha diversity; clinical variables; questionnaire data; Healthy Food Intake Index; KardioKompassi risk; sleep apnea score; stress scores;
782 fitness tests; sleep and activity summaries. The resulting dataset was preprocessed by regressing out the effect of sex and then the effect of age for each variable, only if significantly associated. For the
784 between-individual cross correlation network calculation, the observations were grouped by individual and averaged, obtaining 96 independent observations for each of the 1394 variables. Spearman
786 correlation was calculated for each pair of variables, resulting in 731318 nonmissing estimated ρ coefficients, p-values and Benjamini-Hochberg adjusted p-values (FDR), for the pairs of features of
788 different types (activity and sleep, autoantibody, clinical variables, fitness test, genetic, HFII, KardioKompassi, metabolite, microbial, protein, sleep apnea score, stress score). For the within-
790 individual cross-correlation network calculation, the GWAS scores and the autoantibody data were excluded, resulting in 1058 variables, 96 individuals and 5 time points. We used rmcorr library[58] to
792 estimate the common within-individual association for grouped values measured at the five visits. `rmcorr` estimates a common regression slope representing the association shared among individuals
794 and provides the best linear fit for each individual using parallel regression lines with different intercepts. The repeated-measures correlation coefficient (r_{rm}) is similar to the Pearson correlation
796 coefficient and measures the strength of a linear association but, unlike Pearson correlation, it takes into account non-independence between the measures. Hence, we estimated 347640 nonmissing r_{rm},
798 p-values and Benjamini-Hochberg adjusted p-values (FDR), for the pairs of features of different types

and with at least 100 nonmissing pairs of values. For downstream analysis, we selected the associations satisfying the condition FDR<0.05 and coefficient>0.3 (ρ or r_{rm}) and generated two annotated correlation networks. Communities were extracted with the Louvain method, resulting in modularity values of 0.70 and 0.69 for the between- and within-individuals correlation network respectively.

806

Supplementary Table 1. Characteristics of the study cohort.

	Unit	Value at baseline (n=96)
Age	years (mean ± SE)	40.9 ± 0.9
Sex	counts (M/F)	30/66
BMI	kg/m^2 (mean ± SE)	24.9 ± 0.5
Alcohol consumption	g ethanol/week (mean ± SE)	53.1 ± 5.4
Current smokers[1]	%	16[2]
Education >12 years	%	87
Physical exercise ≥3 times/week	%	56
Married or cohabiting	%	67
Hypercholesterolemia (Total cholesterol >5 mmol/l)	%	44
Hypertriglyceridemia (Females: 20-30 y, >1.5; 30-50 y, >1.7; >50 y, >2 mmol/l Males: 20-30 y, >1.7; >30 y, >2 mmol/l)	%	4
Overweight or obesity (BMI >25 kg/m^2)	%	38
Elevated blood pressure (SBP >130 mmHg)	%	31
Low vitamin D (Serum 25(OH)D <50 nmol/l)	%	31
Hyperglycemia (Fasting blood glucose >6 nmol/l)	%	8
Anemia (Hb <117 (F) or Hb <134 (M) g/l)	%	2
Self-reported obstructive sleep apnea	%	2

808

810

[1] Participants who reported regular smoking were defined as current smokers.

[2] n=94

Supplementary Table 2. List of all the included features and their annotation.

812 (see separate Excel file)

814 **Supplementary Table 3. Results from the GEE model.**

	Estimate	Units	CI	P-value	FDR	Type	# of OORB
Hip circumference	-0.667	cm	-0.957 – -0.377	6.34E-06	8.87E-05	All	1
Serum 25(OH)D	4.072	nmol/l	2.336 – 5.808	4.29E-06	8.87E-05	OORB	24
Systolic blood pressure	-3.078	mmHg	-4.469 – -1.688	1.43E-05	1.33E-04	OORB	27
Diastolic blood pressure	-0.947	mmHg	-1.443 – -0.451	1.81E-04	1.01E-03	OORB	22
Pulse	-3.214	bpm	-4.876 – -1.551	1.52E-04	1.01E-03	OORB	9
Total/HDL cholesterol ratio	-0.405		-0.66 – -0.150	1.88E-03	8.77E-03	OORB	7
LDL cholesterol	-0.085	mmol/l	-0.139 – -0.030	2.21E-03	8.83E-03	OORB	29
ApoB/ApoA1 ratio	-0.014		-0.024 – -0.005	3.89E-03	1.36E-02	OORB	35
Cholesterol	-0.084	mmol/l	-0.145 – -0.024	5.83E-03	1.81E-02	OORB	36

816 **Supplementary Table 4. Associations between MOFA factor values and phenotypic variables.**

818 (see separate Excel file)

Supplementary Table 5. Node and Edge tables for the Between- and Within-Individual Networks.

(see separate Excel file)

824 ## *References*

1. Chen, R. *et al.* Personal omics profiling reveals dynamic molecular and medical
826 phenotypes. *Cell* **148,** 1293–1307 (2012).
2. Chen, R. *et al.* Longitudinal personal DNA methylome dynamics in a human with a
828 chronic condition. *Nat Med* **6,** 1 (2018).
3. Perkins, B. A. *et al.* Precision medicine screening using whole-genome sequencing and
830 advanced imaging to identify disease risk in adults. *Proc Natl Acad Sci USA* **115,** 3686–3691 (2018).
832 4. Piening, B. D. *et al.* Integrative Personal Omics Profiles during Periods of Weight Gain and Loss. *Cell Systems* **6,** 157–170.e8 (2018).
834 5. Price, N. D. *et al.* A wellness study of 108 individuals using personal, dense, dynamic data clouds. *Nat Biotechnol* **35,** 747–756 (2017).
836 6. Zhou, W. *et al.* Longitudinal multi-omics of host-microbe dynamics in prediabetes. *Nature* **569,** 663–671 (2019).
838 7. Schüssler-Fiorenza Rose, S. M. *et al.* A longitudinal big data approach for precision health. *Nat Med* **25,** 792–804 (2019).
840 8. Ahadi, S. *et al.* Personal aging markers and ageotypes revealed by deep longitudinal profiling. *Nat Med* **26,** 83–90 (2020).
842 9. Tebani, A. *et al.* Integration of molecular profiles in a longitudinal wellness profiling cohort. *Nat Commun* **11,** 1–14 (2020).
844 10. Digital Health Revolution. *digitalhealthrevolution.fi* Available at: http://www.digitalhealthrevolution.fi/uploads/2/4/1/5/24155377/person_centric_data_m
846 anagement_models_and_opportunities_in_health_care_sector_full.pdf. (Accessed: 22nd October 2020)
848 11. Argelaguet, R. *et al.* Multi-Omics Factor Analysis—a framework for unsupervised integration of multi-omics data sets. *Mol Syst Biol* **14,** e8124 (2018).
850 12. Argelaguet, R. *et al.* MOFA+: a statistical framework for comprehensive integration of multi-modal single-cell data. *Genome Biology*, **21,** 111 (2020).
852 13. Considine, R. V. *et al.* Serum immunoreactive-leptin concentrations in normal-weight and obese humans. *N Engl J Med* **334,** 292–295 (1996).
854 14. Juge-Aubry, C. E. *et al.* Adipose tissue is a major source of interleukin-1 receptor antagonist: upregulation in obesity and inflammation. *Diabetes* **52,** 1104–1110 (2003).
856 15. Zheng, Z. *et al.* Interacting hepatic PAI-1/tPA gene regulatory pathways influence impaired fibrinolysis severity in obesity. *J. Clin. Invest.* **130,** 4348–4359 (2020).
858 16. Xu, A. *et al.* Adipocyte fatty acid-binding protein is a plasma biomarker closely associated with obesity and metabolic syndrome. *Clinical Chemistry* **52,** 405–413
860 (2006).
17. Fisher, F. M. *et al.* Obesity is a fibroblast growth factor 21 (FGF21)-resistant state.
862 *Diabetes* **59,** 2781–2789 (2010).
18. Mayne, J. *et al.* Associations Between Soluble LDLR and Lipoproteins in a White
864 Cohort and the Effect of PCSK9 Loss-of-Function. *J. Clin. Endocrinol. Metab.* **103,** 3486–3495 (2018).
866 19. Kopchick, J. J., Berryman, D. E., Puri, V., Lee, K. Y. & Jorgensen, J. O. L. The effects of growth hormone on adipose tissue: old observations, new mechanisms. *Nat Rev*
868 *Endocrinol* (2019). doi:10.1038/s41574-019-0280-9
20. Shih, D. M. *et al.* PON3 knockout mice are susceptible to obesity, gallstone formation,
870 and atherosclerosis. *FASEB J.* **29,** 1185–1197 (2015).
21. Nam, S. Y. *et al.* Effect of obesity on total and free insulin-like growth factor (IGF)-1,
872 and their relationship to IGF-binding protein (BP)-1, IGFBP-2, IGFBP-3, insulin, and growth hormone. *Int J Obes* **21,** 355–359 (1997).

22. Meulenberg, P. M. M., Ross, H. A., Swinkels, L. M. J. W. & Benraad, T. J. The effect of oral contraceptives on plasma-free and salivary cortisol and cortisone. *Clinica Chimica Acta* **165,** 379–385 (1987).
23. Barsivala, V., Virkar, K. & Kulkarni, R. D. Thyroid functions of women taking oral contraceptives. *Contraception* **9,** 305–314 (1974).
24. Hodson, L., Skeaff, C. M. & Fielding, B. A. Fatty acid composition of adipose tissue and blood in humans and its use as a biomarker of dietary intake. *Progress in Lipid Research* **47,** 348–380 (2008).
25. Ussher, J. R., Elmariah, S., Gerszten, R. E. & Dyck, J. R. B. The Emerging Role of Metabolomics in the Diagnosis and Prognosis of Cardiovascular Disease. *J. Am. Coll. Cardiol.* **68,** 2850–2870 (2016).
26. Egan, B. M., Greene, E. L. & Goodfriend, T. L. Nonesterified fatty acids in blood pressure control and cardiovascular complications. *Curr. Hypertens. Rep.* **3,** 107–116 (2001).
27. Neiman, M. *et al.* Individual and stable autoantibody repertoires in healthy individuals. *Autoimmunity* **52,** 1–11 (2019).
28. Rubtsova, K., Rubtsov, A. V., Cancro, M. P. & Marrack, P. Age-Associated B Cells: A T-bet-Dependent Effector with Roles in Protective and Pathogenic Immunity. *J Immunol* **195,** 1933–1937 (2015).
29. Prentice, K. J. *et al.* CMPF, a Metabolite Formed Upon Prescription Omega-3-Acid Ethyl Ester Supplementation, Prevents and Reverses Steatosis. *EBioMedicine* **27,** 200–213 (2018).
30. Paige, E. *et al.* Interleukin-6 Receptor Signaling and Abdominal Aortic Aneurysm Growth Rates. *Circ Genom Precis Med* **12,** e002413 (2019).
31. Ristagno, G. *et al.* Pentraxin 3 in Cardiovascular Disease. *Front Immunol* **10,** 1357 (2019).
32. Bonacina, F. *et al.* Pentraxin 3 deficiency protects from the metabolic inflammation associated to diet-induced obesity. *Cardiovasc Res* **115,** 1861–1872 (2019).
33. Wilson, A. M. *et al.* Neuropilin-1 expression in adipose tissue macrophages protects against obesity and metabolic syndrome. *Sci Immunol* **3,** (2018).
34. Frateschi, S. *et al.* PAR2 absence completely rescues inflammation and ichthyosis caused by altered CAP1/Prss8 expression in mouse skin. *Nat Commun* **2,** 161 (2011).
35. Pan, W. & Kastin, A. J. Leptin: a biomarker for sleep disorders? *Sleep Med Rev* **18,** 283–290 (2014).
36. Ishibashi, Y. *et al.* Serum TFF1 and TFF3 but not TFF2 are higher in women with breast cancer than in women without breast cancer. *Sci. Rep.* **7,** 4846 (2017).
37. Floehr, J. *et al.* Association of high fetuin-B concentrations in serum with fertilization rate in IVF: a cross-sectional pilot study. *Hum. Reprod.* **31,** 630–637 (2016).
38. Meex, R. C. *et al.* Fetuin B Is a Secreted Hepatocyte Factor Linking Steatosis to Impaired Glucose Metabolism. *Cell Metab* **22,** 1078–1089 (2015).
39. Zubair, N. *et al.* Genetic Predisposition Impacts Clinical Changes in a Lifestyle Coaching Program. *Sci. Rep.* **9,** 6805 (2019).
40. Walker, C. G. *et al.* Genetic predisposition to an adverse lipid profile limits the improvement in total cholesterol in response to weight loss. *Obesity (Silver Spring)* **21,** 2589–2595 (2013).
41. Okada, Y. & Kamatani, Y. Common genetic factors for hematological traits in humans. *J. Hum. Genet.* **57,** 161–169 (2012).
42. Dopico, X. C. *et al.* Widespread seasonal gene expression reveals annual differences in human immunity and physiology. *Nat Commun* **6,** 7000 (2015).
43. Lakshmikanth, T. *et al.* Human immune system variation during one year. *biorxiv* **17,** 2020.01.22.915025 (2020).
44. Widén, E. & Ripatti, S. Assessment of multifactorial coronary artery disease by utilizing genomic data. *Duodecim* **133,** 776–781 (2017).

45. Niiranen, T. J., Kronholm, E., Rissanen, H., Partinen, M. & Jula, A. M. Self-reported obstructive sleep apnea, simple snoring, and various markers of sleep-disordered breathing as predictors of cardiovascular risk. *Sleep Breath* **20,** 589–596 (2016).
46. Meinilä, J. *et al.* Healthy Food Intake Index (HFII) - Validity and reproducibility in a gestational-diabetes-risk population. - PubMed - NCBI. *BMC Public Health* **16,** 3 (2016).
47. Honko, H. *et al.* W2E--Wellness Warehouse Engine for Semantic Interoperability of Consumer Health Data. *IEEE J Biomed Health Inform* **20,** 1632–1639 (2016).
48. Dressendörfer, R. A., Kirschbaum, C., Rohde, W., Stahl, F. & Strasburger, C. J. Synthesis of a cortisol-biotin conjugate and evaluation as a tracer in an immunoassay for salivary cortisol measurement. *J. Steroid Biochem. Mol. Biol.* **43,** 683–692 (1992).
49. Pruessner, J. C., Kirschbaum, C., Meinlschmid, G.2003. Two formulas for computation of the area under the curve represent measures of total hormone concentration versus time-dependent change. *Elsevier* doi:10.1016/S0306-4530(02)00108-7
50. A, J. *et al.* Extraction and GC/MS analysis of the human blood plasma metabolome. *Anal. Chem.* **77,** 8086–8094 (2005).
51. Schauer, N. *et al.* GC-MS libraries for the rapid identification of metabolites in complex biological samples. *FEBS Lett* **579,** 1332–1337 (2005).
52. Diamanti, K. *et al.* Intra- and inter-individual metabolic profiling highlights carnitine and lysophosphatidylcholine pathways as key molecular defects in type 2 diabetes. *Sci. Rep.* **9,** 1–13 (2019).
53. Hugerth, L. W. *et al.* No distinct microbiome signature of irritable bowel syndrome found in a Swedish random population. *Gut* **69,** 1076–1084 (2020).
54. Hugerth, L. W. *et al.* DegePrime, a program for degenerate primer design for broad-taxonomic-range PCR in microbial ecology studies. *Appl Environ Microbiol* **80,** 5116–5123 (2014).
55. Callahan, B. J. *et al.* DADA2: High-resolution sample inference from Illumina amplicon data. *Nat Meth* **13,** 581–583 (2016).
56. Gagnon-Bartsch, J. A., Jacob, L. & Speed T.P. Removing unwanted variation from high dimensional data with negative controls. (2013). Available at: https://statistics.berkeley.edu/sites/default/files/tech-reports/ruv.pdf (Accessed: 22nd October 2020)
57. Dieterle, F., Ross, A., Schlotterbeck, G. & Senn, H. Probabilistic quotient normalization as robust method to account for dilution of complex biological mixtures. Application in 1H NMR metabonomics. *Anal. Chem.* **78,** 4281–4290 (2006).
58. Bakdash, J. Z. & Marusich, L. R. Repeated Measures Correlation. *Front Psychol* **8,** 456 (2017).

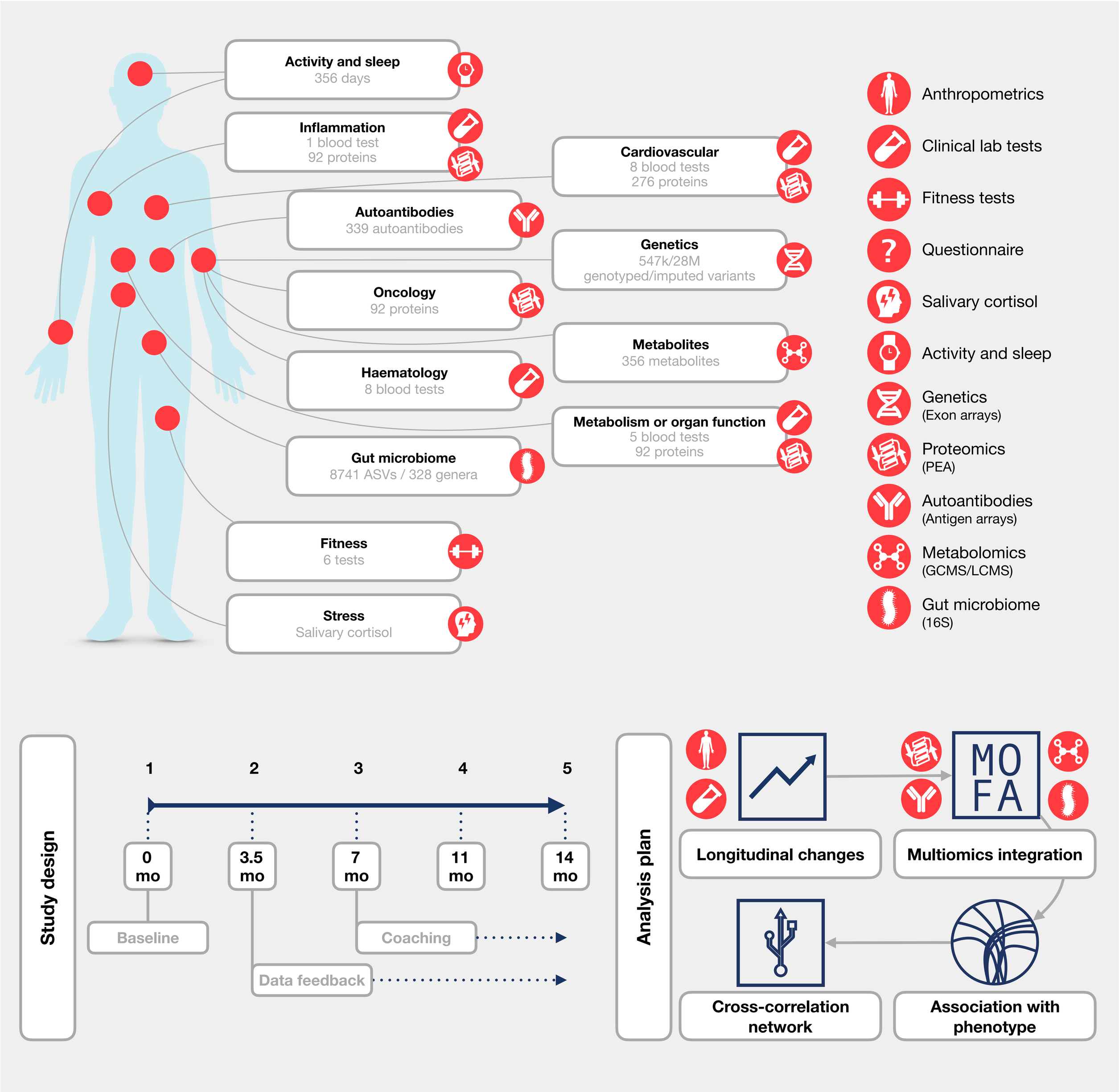

Figure 1: Overview of the measured features, longitudinal design and analysis workflow.

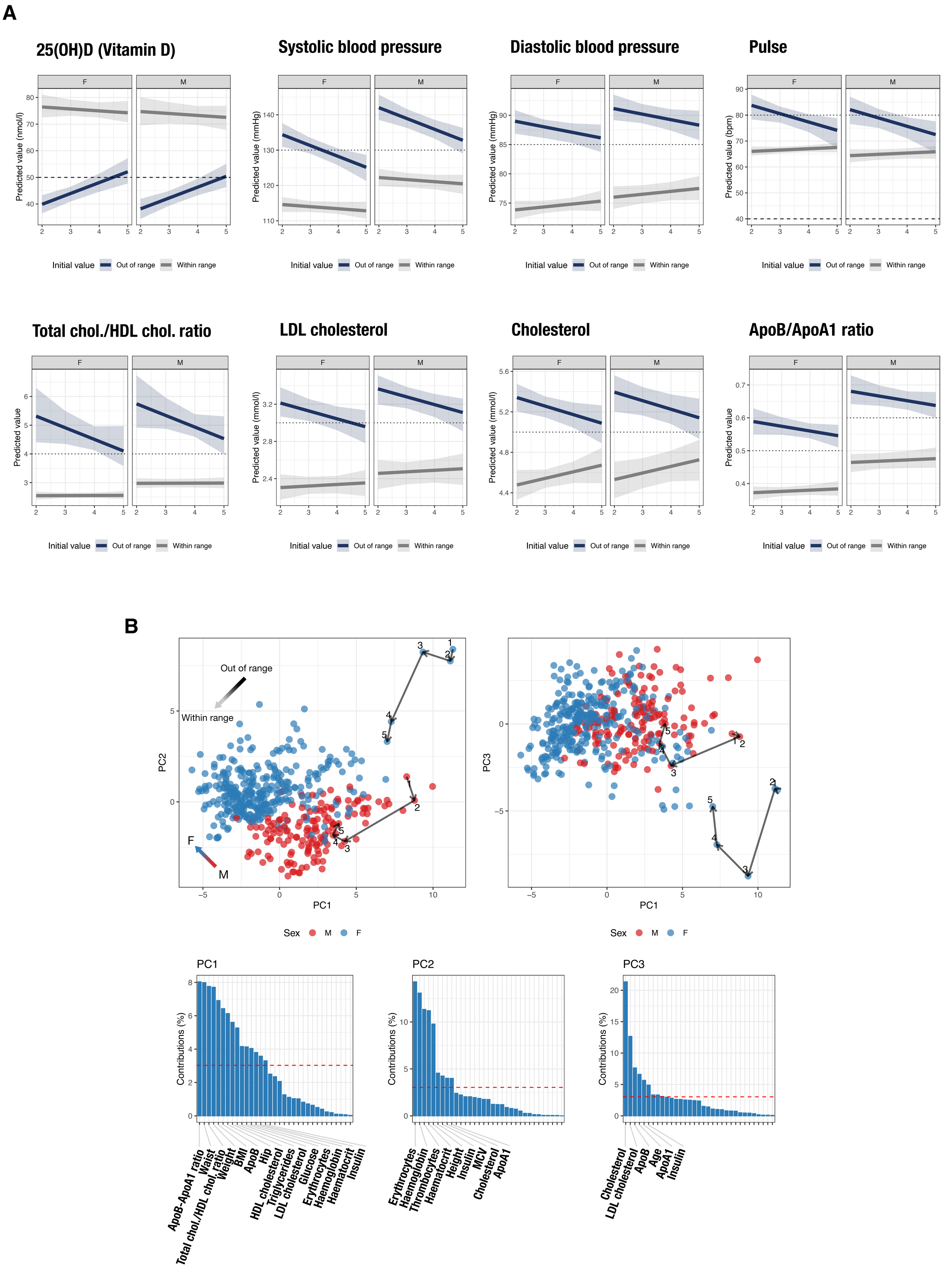
A
25(OH)D (Vitamin D)
Systolic blood pressure
Diastolic blood pressure
Pulse
Total chol./HDL chol. ratio
LDL cholesterol
Cholesterol
ApoB/ApoA1 ratio
F
M
Predicted value (nmol/l)
Predicted value (mmHg)
Predicted value (bpm)
Predicted value
Predicted value (mmol/l)
Initial value
Out of range
Within range
B
Out of range
Within range
PC1
PC2
PC3
Sex
M
F
Contributions (%)
ApoB-ApoA1 ratio
Waist
Total chol./HDL chol. ratio
Weight
BMI
ApoB
Hip
HDL cholesterol
Triglycerides
LDL cholesterol
Glucose
Erythrocytes
Haemoglobin
Haematocrit
Insulin
Erythrocytes
Haemoglobin
Thrombocytes
Haematocrit
Height
Insulin
MCV
Cholesterol
ApoA1
Cholesterol
LDL cholesterol
ApoB
Age
ApoA1
Insulin

Figure 2: A. Longitudinal analysis reveals the positive effect of data feedback and coaching on health. Generalized Estimating Equation (GEE) model prediction for the significantly changed variables (FDR<0.05), stratified by sex and out/within range status at baseline. For this analysis, the second visit represented a baseline because data feedback and coaching started at the 2nd and 3rd visits respectively (grey: within range, blue: out of range). Bootstrapped confidence intervals are shown. **B.** Principal components plot of the individuals obtained using all the numerical clinical variables. The trajectories for two selected individuals along successive study visits are shown with arrows. The loadings for the first three PCs are shown in the bottom panels and the variables with relative contribution higher than average (red line) are named.

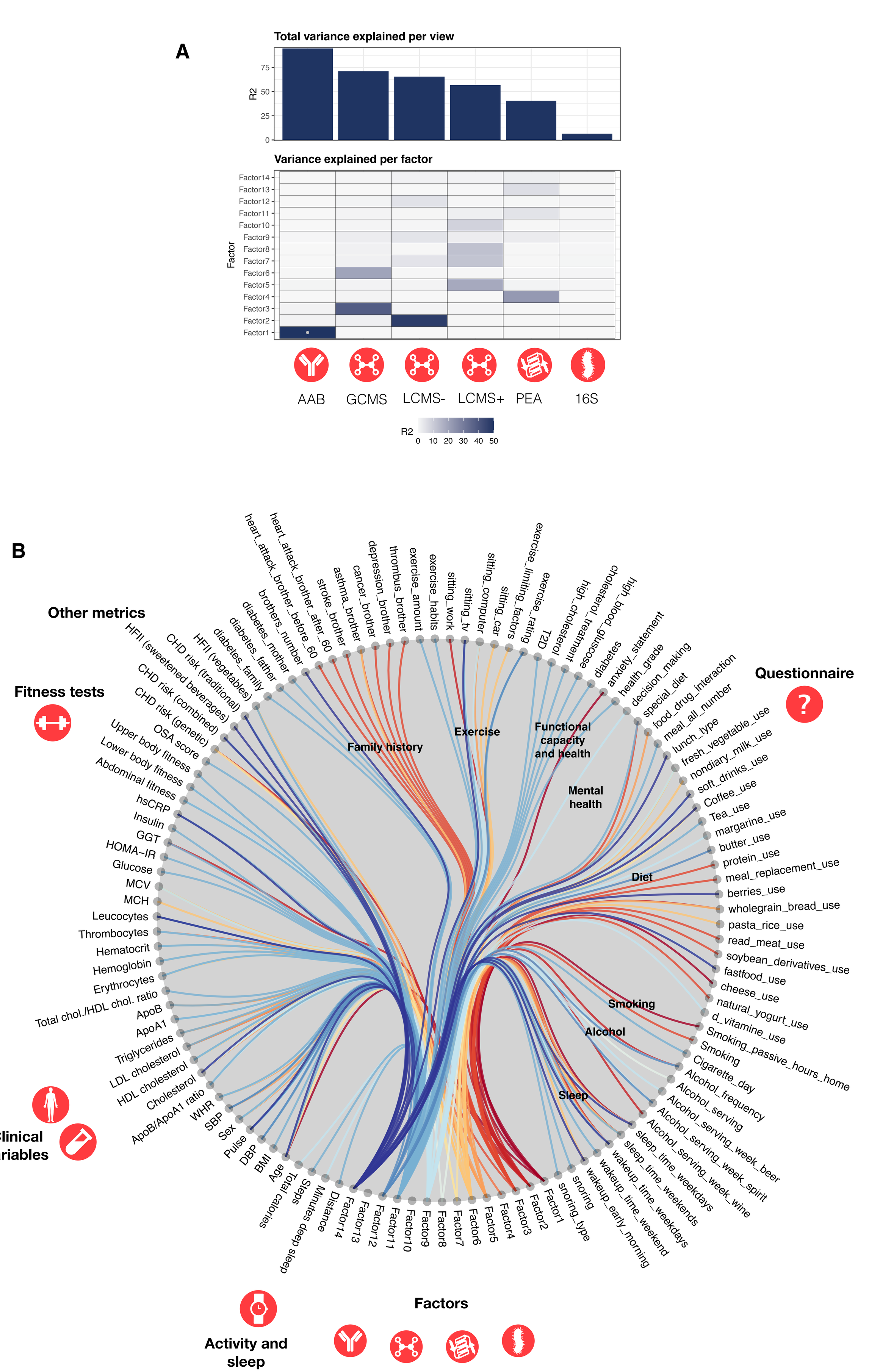
A
Total variance explained per view
R2
75
50
25
0
Variance explained per factor
Factor
Factor14
Factor13
Factor12
Factor11
Factor10
Factor9
Factor8
Factor7
Factor6
Factor5
Factor4
Factor3
Factor2
Factor1
AAB
GCMS
LCMS-
LCMS+
PEA
16S
R2
0 10 20 30 40 50
B
Other metrics
Fitness tests
Clinical variables
Activity and sleep
Factors
Questionnaire
Family history
Exercise
Functional capacity and health
Mental health
Diet
Smoking
Alcohol
Sleep
HFII (sweetened beverages)
CHD risk (traditional)
CHD risk (combined)
CHD risk (genetic)
HFII (vegetables)
OSA score
diabetes_family
Upper body fitness
diabetes_father
Lower body fitness
diabetes_mother
Abdominal fitness
diabetes_number
hsCRP
brothers_number
Insulin
heart_attack_brother_after_60
GGT
heart_attack_brother_before_60
HOMA–IR
stroke_brother
Glucose
asthma_brother
MCV
cancer_brother
MCH
depression_brother
Leucocytes
thrombus_brother
Thrombocytes
exercise_amount
Hematocrit
exercise_habits
Hemoglobin
sitting_work
Erythrocytes
sitting_tv
Total chol./HDL chol. ratio
sitting_computer
ApoB
sitting_car
ApoA1
exercise_limiting_factors
Triglycerides
exercise_rating
LDL cholesterol
T2D
HDL cholesterol
high_cholesterol_treatment
Cholesterol
high_blood_glucose
ApoB/ApoA1 ratio
diabetes
WHR
anxiety_statement
SBP
health_grade
Sex
decision_making
Pulse
special_diet
DBP
food_drug_interaction
BMI
meal_all_number
Age
lunch_type
Total calories
fresh_vegetable_use
Steps
nondiary_milk_use
Minutes deep sleep
soft_drinks_use
Distance
Coffee_use
Factor14
Tea_use
Factor13
margarine_use
Factor12
butter_use
Factor11
protein_use
Factor10
meal_replacement_use
Factor9
berries_use
Factor8
wholegrain_bread_use
Factor7
pasta_rice_use
Factor6
read_meat_use
Factor5
soybean_derivatives_use
Factor4
fastfood_use
Factor3
cheese_use
Factor2
natural_yogurt_use
Factor1
d_vitamine_use
snoring_type
Smoking_passive_hours_home
snoring
Smoking
wakeup_early_morning
Cigarette_day
wakeup_time_weekend
Alcohol_frequency
wakeup_time_weekdays
Alcohol_serving
sleep_time_weekends
Alcohol_serving_week_beer
sleep_time_weekdays
Alcohol_serving_week_spirit
Alcohol_serving_week_wine

Figure 3. A. Variance decomposition. Percentage of total variance explained (R^2) for each data layer (up) or variance explained (R^2) for each factor and data layer (bottom). A dot marks the out-of-bound value (>50%) for autoantibodies. **B.** Association with phenotype. The factor values were tested for their association with the phenotypic variables and the top associations (FDR<0.001) are shown. The edges are bundled according to their category and colored based on the originating factor.

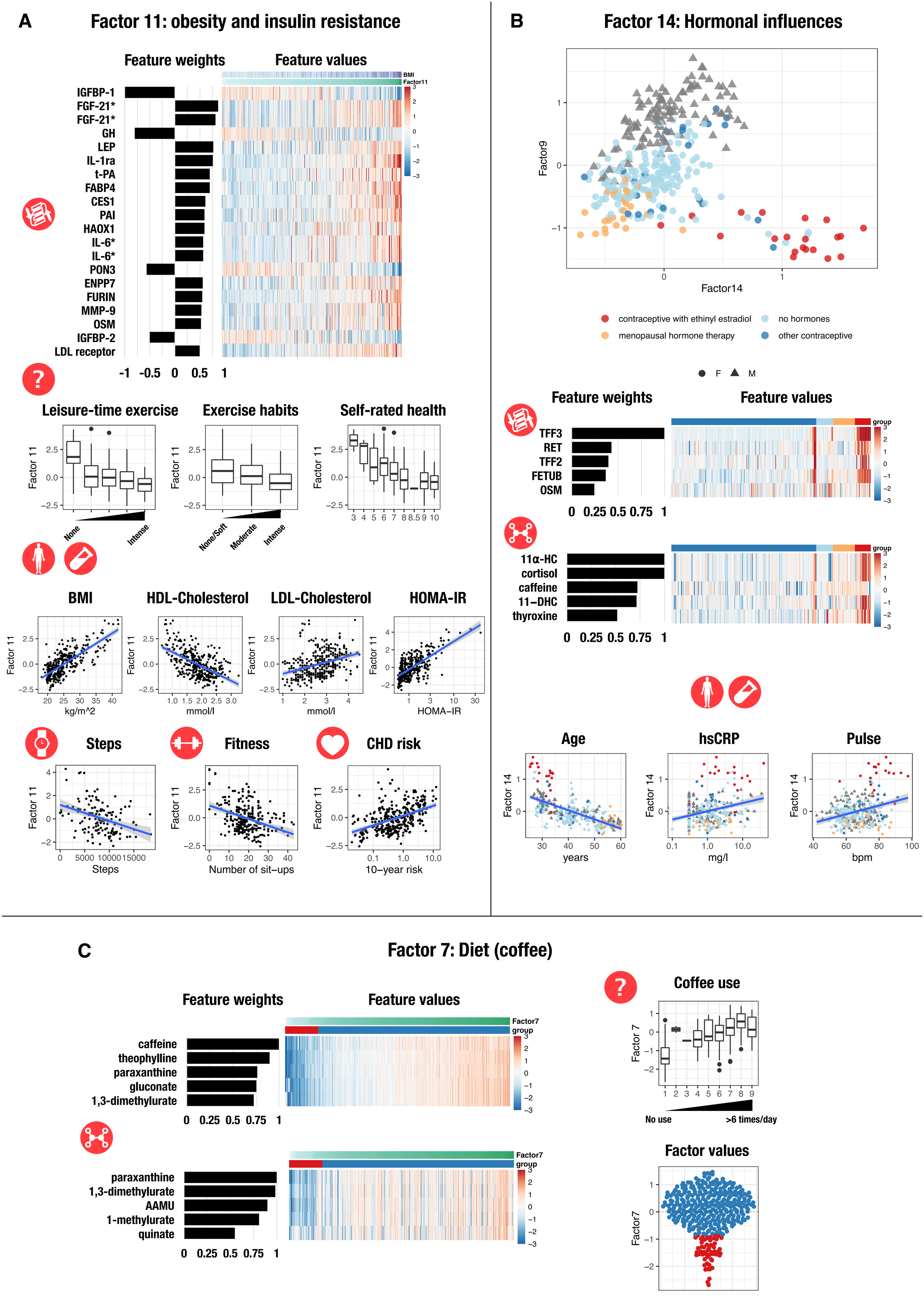
A
Factor 11: obesity and insulin resistance
Feature weights
Feature values
BMI
Factor11
IGFBP-1
FGF-21*
FGF-21*
GH
LEP
IL-1ra
t-PA
FABP4
CES1
PAI
HAOX1
IL-6*
IL-6*
PON3
ENPP7
FURIN
MMP-9
OSM
IGFBP-2
LDL receptor
-1 -0.5 0 0.5 1
Leisure-time exercise
None
Intense
Exercise habits
None/Soft
Moderate
Intense
Self-rated health
BMI
kg/m^2
HDL-Cholesterol
mmol/l
LDL-Cholesterol
mmol/l
HOMA-IR
Steps
Steps
Fitness
Number of sit–ups
CHD risk
10–year risk
Factor 11
B
Factor 14: Hormonal influences
Factor9
Factor14
contraceptive with ethinyl estradiol
no hormones
menopausal hormone therapy
other contraceptive
F
M
Feature weights
Feature values
group
TFF3
RET
TFF2
FETUB
OSM
0 0.25 0.5 0.75 1
11α-HC
cortisol
caffeine
11–DHC
thyroxine
Age
years
hsCRP
mg/l
Pulse
bpm
Factor 14
C
Factor 7: Diet (coffee)
Feature weights
Feature values
Factor7
group
caffeine
theophylline
paraxanthine
gluconate
1,3-dimethylurate
0 0.25 0.5 0.75 1
paraxanthine
1,3-dimethylurate
AAMU
1-methylurate
quinate
Coffee use
Factor 7
No use
>6 times/day
Factor values
Factor7

Figure 4. A. Factor 11 is linked to obesity and insulin sensitivity. The top scaled protein weights for Factor 11 are shown as well as their values (row z-score). The association between the factor values for each sample and the phenotypic variables is shown. A regression line with 95% confidence interval is shown when appropriate. An asterisk marks the proteins measured on multiple PEA panels. **B.** Factor 14 is influenced by hormones. A scatterplot of Factor 9 and Factor 14 values shows that samples can be separated based on the sex (Factor 9) and the use of hormones (Factor 14). Factor 14 identifies a group of young women using contraceptives with ethinyl estradiol (red). The top metabolites and proteins with positive scaled weights on Factor 14 are shown. The original feature values are shown as a heatmap (row z-score). The association between the factor values for each sample and the phenotypic variables is shown, as well as a regression line with 95% confidence interval. Points are coloured as in the top panel. Abbreviations: 11α-HC: 11alpha–hydrocortisone, 11–DHC: 11–dehydrocorticosterone. **C.** Factor 7 is associated to coffee consumption. The scaled positive weights are shown for the top metabolites, as well as their values. The association between the factor values with self-reported coffee consumption is shown. A two-group classification of the samples based on Factor 7 values was obtained with gaussian-mixture modeling and shown with colored dots (red: lower coffee consumption, blue: higher coffee consumption).

A Between-individuals

Cardiometabolic

PAPPA
AR
PAI
FABP4
SEZ6L
Distance
Gal-9
Steps
hsCRP
NPTXR
CLMP
KYAT1
Hip
1-arachidoyl-GPC (20...
1-docosapentaenoyl-G...
Total calories
Waist
PAF (18:0)
Cysteine, S-methyl-,...
Pulse
Weight
TYROSINE
BMI
OSA score
IGFBP-1
Lachnospiraceae_Copr...
SERINE
Upper body fitness
t-PA
RTN4R
IL1RL2
Intense activities
ALCAM
PON3
Abdominal fitness
MERTK
FETUB
IL-1ra
CITRIC ACID
LEP
IGFBP-2
2-palmitoyl-GPE* (16...
OSM
RARRES2
PRSS8
FURIN
CES1
LDL-receptor
1-pentadecanoylglyce...
Lower body fitness
alpha-CEHC
CHI3L1
CTSD
CDHR5
PAF(12:0)
CD164
1-palmitoylplasmenyl...
LOX-1
ApoA1
1-stearoylplasmenyle...
Insulin
SERPINA7
thyroxine
HDL cholesterol
1-myristoyl-GPC (14:...
CPE
NOMO1
Total chol./HDL chol...
Hypoxanthine
PAF (14:1)
ERBB3
TRAIL
MMP-9
Leucocytes
Triglycerides
palmitoleoyl-GPC* (1...
PLTP
ApoB/ApoA1 ratio
1-eicosatrienoyl-GPC...
APOM
CCL16
TRAIL
gamma-glutamylalanin...
ApoB
F7
Notch-3
1-eicosapentaenoylgl...
TNFSF14
SERPINA5
Hydroxyoctadecenoyl-...
2-arachidonoyl-GPE* ...
PLA2G7
SCGB3A2
PCSK9
uPA
MMP-2
LILRA5
gamma-glutamylleucin...
PROC
BMP-6
CHD risk (combined)
PTPRS
uPA
Cholesterol
CHOLESTEROL
CFHR5
aspartylleucine
Hydroxyisovaleroylca...
TR-AP
FCN2
3-Carboxy-4-methyl-5...
alpha-Tocopherol
Hydroxylauroyl-carni...
LDL cholesterol
Beta-alanine
1-linoleoyl-GPE (18:...
Protein C levels
LAMP2_aAb
Lipoprotein phosphol...
TWEAK
TFPI
LDL cholesterol
SOX10_aAb

B Within-individuals

Activity and sleep

GLYCEROL-3-PHOSPHATE
Cholesta-3,5-diene
Minutes in bed
SOST
Defluviitaleaceae_De...
Laurylcarnitine (C12...
2-Hydroxyoctanoate
Weight
Octanoyl-carnitine (...
Glutarylcarnitine (C...
Minutes deep sleep
1-myristoyl-GPC (14:...
Minutes awake
3-Hydroxydecanoate
Calories
beta-D-Glucopyranose
Carnitine
Moderate activities
PAF(12:0)
LEP
cis-4-decenoyl carni...
Dodecenoyl-carnitine...
Rhodospirillaceae_NA
Steps
leucylglycine
Eicosadieneoyl-carni...
PRSS8
Hydroxyisovaleroylca...
Soft activities
3-HYDROXYBUTYRIC ACI...
Decanoylcarnitine (C...
NRP1
Tetradecadienyl-carn...
BMI
Minutes light sleep
1-nonadecanoylglycer...
Distance
Myristoleoylcarnitin...
SCGB3A2
Oleoylcarnitine (C18...
Intense activities
Acetylcarnitine (C2:...
Hexadecenoyl-carniti...
THBS4
IDUA
PTX3
Uracil
Myristoylcarnitine (...
citrulline
LPL
Butyrylcarnitine (C4...
THREONINE
OCTADECENOIC ACID,-9...
TLT-2
5-acetylamino-6-amin...
Hydroxyoctadecenoyl-...
Hydroxymyristoyl-car...
Hydroxylauroyl-carni...
(R*,S*)-2,3-Dihydrox...

Inflammation

TNF-R2
TNFSF13B
CD160
IL-12B
GZMB
kynurenine
XCL1
IL-18BP
5-hydroxyindoleaceta...
IL-10
CXCL9
2-oxindole-3-acetate
CCL3
CEACAM8
ITGAV
OSM
HGF
CCL24
CDCP1
CXCL10
IL2-RA
TNFRSF6B
IL-6
SERPINA5
Gal-9
CXCL11
Malic acid
HGF
IL-6
hsCRP
MIP-1-alpha
Citric acid
FABP4
Hypoxanthine
Leucocytes
PRTN3
HDL cholesterol
IL-1ra
CCL4
PGLYRP1
CTSV
CPE
NADK
MPO
MCP-2
COMP
Protein-BOC
IL27
CSF-1
LOX-1
MMP-9
VEGF-A
CYR61
MMP-10
Pulse
riboflavin (Vitamin ...

Data type (node color)

- Proteins
- Metabolites
- Biometrics
- Genetic scores
- Autoantibodies
- Activities and sleep
- Gut microbiome
- Other

Correlation (edge color)

- +

Figure 5. Cross-correlation network analysis aids the interpretation the relationship between data types. Only associations between features of different type were considered to calculate correlation networks at FDR<0.05. The size of the nodes is proportional to the node degree and the edge thickness is proportional to the magnitude of the correlation. The node color indicate different data types. The proteins appearing twice in the network were measured on multiple PEA panels. **A.** Selected between-individual subnetwork. **B**. Selected within-individual network modules.

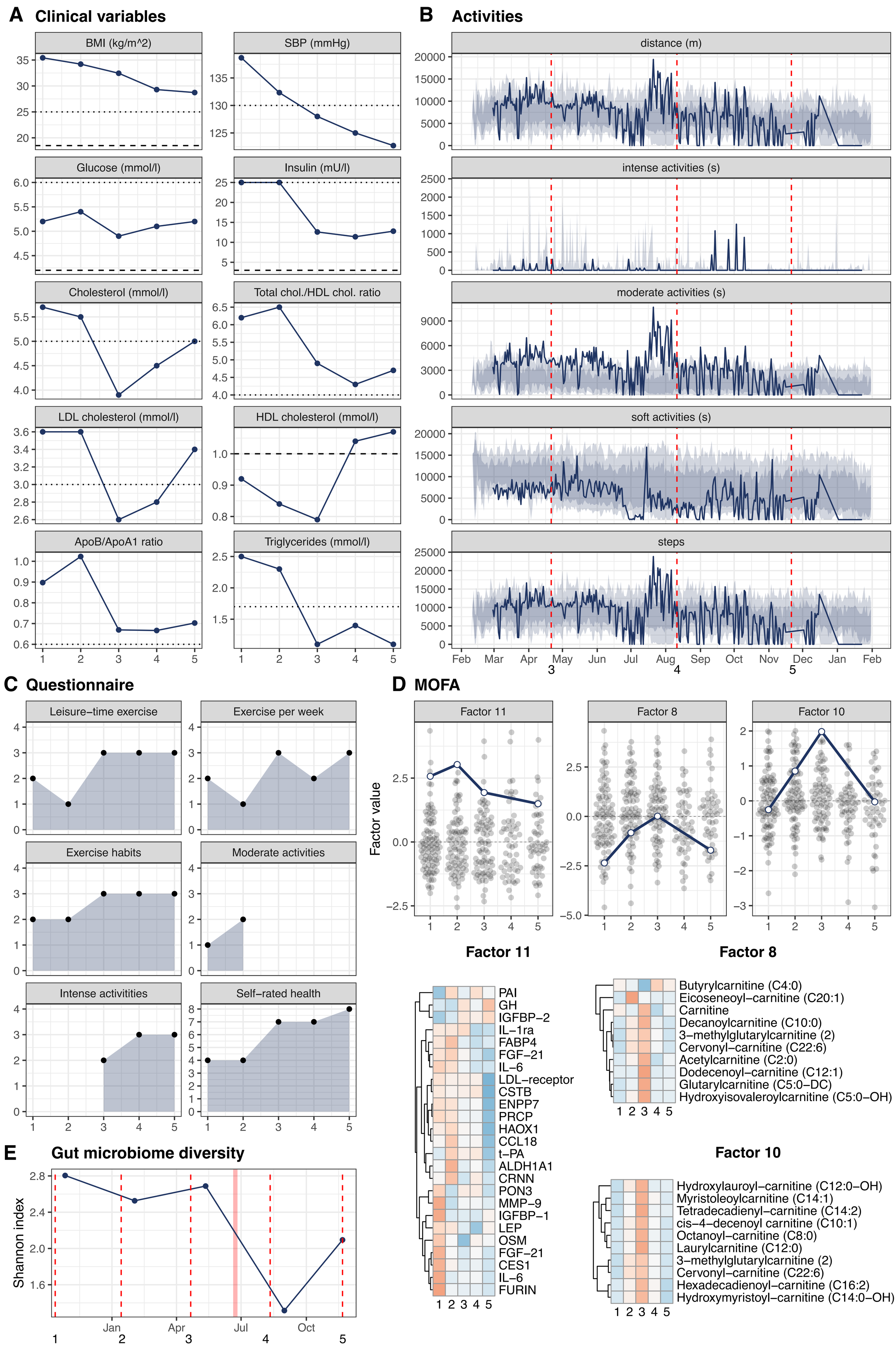
A Clinical variables
BMI (kg/m^2)
SBP (mmHg)
Glucose (mmol/l)
Insulin (mU/l)
Cholesterol (mmol/l)
Total chol./HDL chol. ratio
LDL cholesterol (mmol/l)
HDL cholesterol (mmol/l)
ApoB/ApoA1 ratio
Triglycerides (mmol/l)
B Activities
distance (m)
intense activities (s)
moderate activities (s)
soft activities (s)
steps
Feb Mar Apr May Jun Jul Aug Sep Oct Nov Dec Jan Feb
C Questionnaire
Leisure−time exercise
Exercise per week
Exercise habits
Moderate activities
Intense activitities
Self−rated health
D MOFA
Factor 11
Factor 8
Factor 10
Factor value
PAI
GH
IGFBP−2
IL−1ra
FABP4
FGF−21
IL−6
LDL−receptor
CSTB
ENPP7
PRCP
HAOX1
CCL18
t−PA
ALDH1A1
CRNN
PON3
MMP−9
IGFBP−1
LEP
OSM
FGF−21
CES1
IL−6
FURIN
Butyrylcarnitine (C4:0)
Eicoseneoyl−carnitine (C20:1)
Carnitine
Decanoylcarnitine (C10:0)
3−methylglutarylcarnitine (2)
Cervonyl−carnitine (C22:6)
Acetylcarnitine (C2:0)
Dodecenoyl−carnitine (C12:1)
Glutarylcarnitine (C5:0−DC)
Hydroxyisovaleroylcarnitine (C5:0−OH)
Hydroxylauroyl−carnitine (C12:0−OH)
Myristoleoylcarnitine (C14:1)
Tetradecadienyl−carnitine (C14:2)
cis−4−decenoyl carnitine (C10:1)
Octanoyl−carnitine (C8:0)
Laurylcarnitine (C12:0)
3−methylglutarylcarnitine (2)
Cervonyl−carnitine (C22:6)
Hexadecadienoyl−carnitine (C16:2)
Hydroxymyristoyl−carnitine (C14:0−OH)
E Gut microbiome diversity
Shannon index
Jan Apr Jul Oct

Figure 6. A case study: lifestyle change in one individual and the associated molecular changes. **A.** Clinical variables showing longitudinal changes. Reference values are shown (dashed line: lower normal value, dotted line: upper normal value) **B.** Daily summary of the activities recorder by the smart watch included: distance, time spent in intense, moderate or soft activities and number of steps. The shaded area correspond to the 10, 25, 75 and 90 percentiles in the whole population. The study visits are marked with vertical dashed lines **C.** Selected lifestyle questions. The numbers correspond to orderer categories, where a higher number corresponds to higher frequency or more favorable outcome. **D.** Longitudinal values for selected MOFA+ factors (blue line) plotted together with the factor values for the remaining samples at each study visit (grey dots). The top features for the corresponding factors are shown as heatmaps (row z-score, blue:low, red:high). **E.** Gut microbiome diversity (Shannon index). The vertical dashed line mark the date for the study visit, which could be different than the fecal sample collection date (dots). A red shaded area mark a period of antibiotic treatment.